

Optimal Mechanisms for Demand Response: An Indifference Set Approach

Mohammad Mehrabi
mehrabi@stanford.edu

Omer Karaduman
omerkara@stanford.edu

Stefan Wager
swager@stanford.edu

Draft version September 13, 2024

Abstract

The time at which renewable (e.g., solar or wind) energy resources produce electricity cannot generally be controlled. In many settings, consumers have some flexibility in their energy consumption needs, and there is growing interest in demand-response programs that leverage this flexibility to shift energy consumption to better match renewable production—thus enabling more efficient utilization of these resources. We study optimal demand response in a model where consumers operate home energy management systems (HEMS) that can compute the “indifference set” of energy-consumption profiles that meet pre-specified consumer objectives, receive demand-response signals from the grid, and control consumer devices within the indifference set. For example, if a consumer asks for the indoor temperature to remain between certain upper and lower bounds, a HEMS could time use of air conditioning or heating to align with high renewable production when possible. Here, we show that while price-based mechanisms do not in general achieve optimal demand response, i.e., dynamic pricing cannot induce HEMS to choose optimal demand consumption profiles within the available indifference sets, pricing is asymptotically optimal in a mean-field limit with a growing number of consumers. Furthermore, we show that large-sample optimal dynamic prices can be efficiently derived via an algorithm that only requires querying HEMS about their planned consumption schedules given different prices. We demonstrate our approach in a grid simulation powered by OpenDSS, and show that it achieves meaningful demand response without creating grid instability.

1 Introduction

Consumer electricity demand is largely unmanaged. In most markets today, consumers obtain electricity via fixed-rate contracts that do not adapt to real-time grid conditions or reflect the true costs of electricity production. This unmanaged demand is in tension with renewable energy resources, such as solar and wind: Unlike conventional energy resources, renewables yield intermittent production and cannot be dispatched on demand, thus leading to frequent mismatches between electricity production and consumption [Gowrisankaran et al., 2016, Cordera et al., 2023]. This supply-demand mismatch then often forces the grid to depend on expensive and less efficient power plants during peak demand periods, leading to increased operational expenses and environmental impacts [Bird et al., 2013, Impram et al., 2020, Michaelides, 2019].

We are grateful to Andrey Bernstein, Mahmoud Saleh and Xinyang Zhou for valuable feedback and numerous helpful conversations; and also thank Xinyang Zhou for helping us get set up with the OpenDSS grid simulator. This research was funded by a grant from Trellis Climate (Prime Coalition) to advance deep demand flexibility solutions and a grant from the Office of Naval Research.

As renewable energy sources like solar and wind become more prevalent—for example, in the U.S., electricity demand is expected to grow by approximately 1% annually from 2022 to 2050, with renewable sources projected to supply 44% of electricity by 2050, up from 21% in 2021 [U.S. Energy Information Administration, 2023]—these inefficiencies are projected to intensify further, mainly due to the mismatch between renewable energy availability and peak demand periods. This mismatch is exacerbated by the growing adoption of rooftop solar panels, which allow households to both generate and consume electricity, thereby causing local demand profiles to fluctuate unpredictably. These fluctuations require more sophisticated balancing mechanisms to maintain grid stability Caballero-Pena et al. [2022], highlighting the need for more adaptive and responsive demand management solutions.

To address this challenge, demand-response programs have gained attention by leveraging user flexibility [Yoon et al., 2014, Godina et al., 2018, Siano, 2014]. For example, demand response may involve pre-cooling: On a hot day, it may be advantageous to apply air conditioning early in the afternoon while solar production is plentiful, thus enabling reduced electricity consumption during evening peak hours. However, real-world implementations of demand response programs have encountered significant limitations.

In California, the state’s grid operator has deployed text message alerts to urge residents to reduce electricity use during peak demand periods, especially during extreme heat waves. While this method effectively prompts immediate public action, it relies heavily on voluntary participation and may not consistently achieve predictable load reductions. Specifically, according to the 2022 Flex Alert Marketing, Education & Outreach (ME&O) Effectiveness Study [Opinion Dynamics, 2024], 93% of Californians did not have a complete and accurate understanding of all aspects of the Flex Alert program in 2022, an initiative designed to encourage voluntary electricity conservation during periods of high energy demand.

In Texas, a more advanced system has been introduced where consumers are incentivized to lower their energy usage relative to a predetermined baseline. This program, known as the *Emergency Response Service*, compensates participants for curtailing electricity use during grid emergencies. However, there have been concerns about the program’s fairness and effectiveness due to potential manipulation by strategic consumers [Office of Science and Technology Policy, 2022]; for example, some cryptocurrency miners have been accused of inflating their baseline consumption to maximize payouts when reducing usage.

These examples illustrate the challenges in designing demand-response programs that are both effective in managing grid costs and robust against adversarial behaviors, highlighting the need for more sophisticated demand-response management strategies.

1.1 Demand Response with Home Energy Management Systems

Home Energy Management Systems (HEMS) offer a robust solution for automating household energy management by dynamically adjusting consumption plans in response to grid conditions and demand-response signals, demonstrating significant potential for improving demand-response strategies. These systems allow users to set preferences, such as desired indoor temperature ranges, and then operate devices to meet these preferences while optimizing energy use [Beaudin and Zareipour, 2015, Zhou et al., 2016]. By interacting directly with the grid, HEMS can pre-cool or pre-heat homes when renewable energy is abundant, reducing demand during peak periods without compromising comfort. This approach enhances grid flexibility and efficiency seamlessly, without placing impractical decision-making burdens on users [Faruqui et al., 2010].

The first fundamental question that arises when implementing demand-response systems with HEMS is: What kind of demand flexibility can the HEMS exploit? In full generality, one could imagine each customer writing down a complete welfare function and then having the HEMS optimize it; and this is the standard starting point in most of the existing literature [Adelman and Uçkun, 2019, Zhou et al., 2017]. Consumers have a documented willingness of, e.g., refraining from washing clothes in response to higher prices during peak hours [Allcott, 2011a]. Furthermore, this type of HEMS could in principle navigate complex tradeoffs: For example, some consumers may be willing to sell the energy stored in their EV battery (and forgo transportation) when prices are high, while other may be willing to set adaptive indoor temperature targets depending on prices. In practice, however, there’s likely a limit to how well consumers can directly reason about welfare implications of energy use choices in the face of fluctuating energy prices because of to the high required cognitive costs [Friedman and Oren, 1995, Hobman et al., 2016].

In this paper, we instead focus on a narrower form of demand response, which does not seek to shape consumer behavior and instead simply leverages under-specification in the consumers’ existing preferences. Perhaps a consumer wants their EV charged by morning—but doesn’t care exactly when the charging happens; or perhaps a consumer sets upper and lower bounds on a thermostat, but doesn’t care how the indoor temperature evolves between these bounds. We model this underspecification as leading to indifference sets containing a number of equally desirable energy consumption profiles; and consider the demand response problem in which we seek to induce the HEMS to pick consumption profiles from within the indifference set in a way that is well aligned with overall grid objectives.

Given this formulation of the demand response problem, the second fundamental question is: What kind of signals should the grid send to the HEMS to achieve optimal demand response? At one extreme, a decentralized system could be implemented where the grid uses dynamic pricing, and the HEMS simply seek to minimize costs while meeting user preferences. At the other extreme, in a fully centralized system, the HEMS could give the grid transparent control over all devices, allowing the grid to solve a global optimization problem. We refer to these two mechanisms as the (dynamic) pricing mechanism and the direct control mechanism. We study both mechanisms, and seek to understand how close the pricing mechanism can get to direct control in terms of demand response metrics. In particular, we show the following:

1. Under our indifference-set model for demand response, the pricing mechanism described above is generally not optimal relative to the direct control mechanism. A grid operator with direct control of all consumer devices can achieve better demand response (while respecting user indifference sets) than an operator who can only control demand via dynamic prices.¹
2. As the market size increases, the optimality gap of pricing mechanisms shrinks to zero. In the mean-field limit with infinitely many customers, the grid cost for both pricing and direct control mechanisms converge, and the price-based mechanisms becomes optimal.
3. Mean-field optimal prices can be recovered via a first-order algorithm that only requires querying HEMS about planned consumption profiles at different price levels, as these consumption

¹This finding may seem surprising at first glance, as there are numerous welfare theorems in economics demonstrating that price-based mechanisms can achieve optimal welfare in various systems [Mas-Colell et al., 1995]. Our indifference-set model, however, is inconsistent with a key assumption of these welfare theorems, often referred to as local non-satiation. Local non-satiation implies that consumer demand moves smoothly with prices—but this is not the case here, as in our setting we only consider hard constraints on the user side.

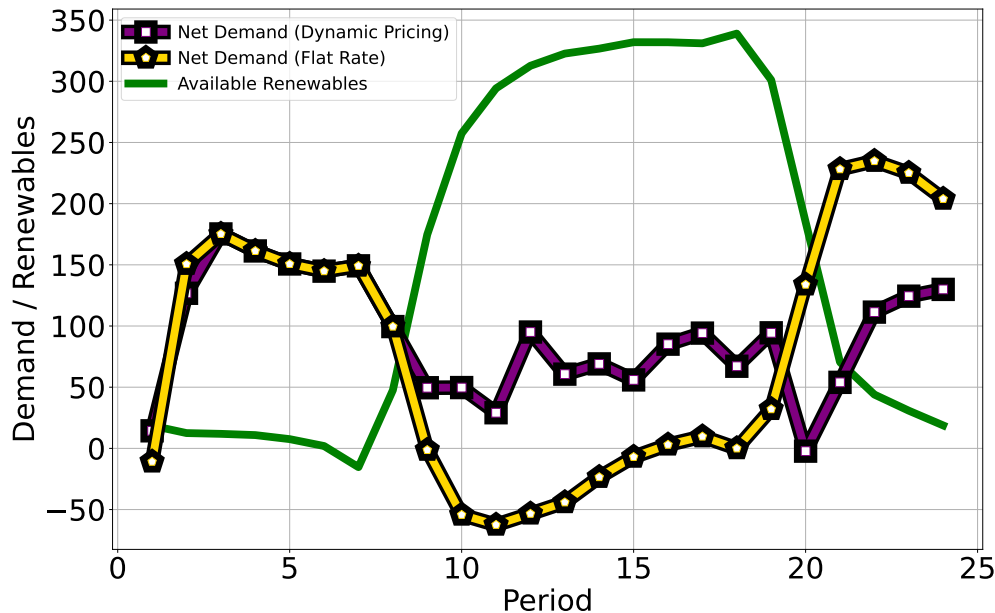


Figure 1: Impact of optimized dynamic pricing on the net demand curve—demand minus available renewables—in the household cooling case study in Phoenix, Arizona (see Section 5). By transitioning from flat-rate pricing to the selected dynamic pricing, the classic “duck-shaped” net demand curve has been effectively flattened. The traditional duck curve, which represents net demand under flat-rate pricing, is problematic due to significant fluctuations from early morning (high demand/low renewables) to midday (low demand/high renewables) and again from midday to late evening (high demand/low renewables). The dynamic pricing applied in this study was derived solely from querying HEMS regarding their consumption profiles in response to various pricing signals.

profiles give information about a dual cost function. This allows for the straightforward application of first-order optimization methods to find the optimal price using only market-level data, without the grid needing to directly query for individual user preferences.

Finally, we demonstrate practical promise of our pricing approach on a grid-simulation motivated by pre-cooling with data from Phoenix, Arizona; we use OpenDSS to solve the relevant power-flow equations. As seen in Figure 1, renewable production is heavily concentrated during daytime hours. With flat rates, this results in the notorious “duck curve” with low (even negative) net demand during the day that then quickly ramps up in the evening.² In contrast, our proposed algorithm shifts demand earlier into the day when solar resources are plentiful, thus enabling it to reduce load in the evening hours. We give further details on this experiment in Section 5.

1.2 Related work

As the demand for electricity continues to rise and the efficiency and environmental benefits of renewable energy sources grow, there has been significant interest in demand-response programs. Demand response programs are generally classified into two main categories: Dynamic pricing and

²One should imagine the ramp-up period as forming the neck of the duck and the evening peak demand its head [Denholm et al., 2015].

incentive-based programs. The former use time-varying prices to better align demand with supply [Adelman and Uçkun, 2019, Peura and Bunn, 2015, Uçkun, 2012, Crew et al., 1995], while the later involves compensating users through specific contracts to adhere to designated consumption patterns during certain time windows.

Pricing-based mechanisms for demand response are typically framed as Stackelberg games with a two-level leader-follower structure [Adelman and Uçkun, 2019, Zhou et al., 2017, 2019]: First the grid sets prices, and then consumers respond to these prices. Our indifference-set approach is a special case of such a Stackelberg games, where lower-level optimization involves consumers choosing their energy consumption to minimize costs while remaining within their indifference sets (i.e., the consumer preferences are instantiated as hard constraints on allowed consumption patterns). We note that Stackelberg games are also often used for the more abstract task of policy learning with strategic agents [Chen et al., 2020, Munro, 2024, Perdomo et al., 2020, Sahoo and Wager, 2022]; and our paper can be seen as a part of this broader literature that exploits specific structure of consumer energy price response.

Perhaps closest to us in the literature on price-based mechanisms, Adelman and Uçkun [2019] study dynamic pricing in a setting that includes current energy demand, appliance status, operation times, global variables such as weather conditions, among many others. They assume that each consumer’s welfare depends on their energy usage in a differentiable way, and that consumers choose their energy consumption to optimize welfare in response to set prices (e.g., using a HEMS). Given this setup, the authors define the social planner’s welfare function as the sum of all consumers’ welfare minus the grid’s generation cost, and seek prices that optimize the social planner’s welfare under the posited consumer behavior model (the consumers choose how much to consume in response to prices, and the grid must then meet this demand). Their main result is that, as the system size grows large, the optimal price mechanism in their model is one that perfectly externalizes the grid’s incremental production costs to the consumers, i.e., in equilibrium, energy is priced to match the marginal cost of production. The authors propose finding prices that maximize the social planner’s welfare via a tempered fixed-point iteration algorithm.

Like Adelman and Uçkun [2019], we consider a model where—at least in a qualitative sense—prices are set in the view of mutual benefit of consumers and producers. However, unlike Adelman and Uçkun [2019], we do not rely on properties of the consumer welfare function, and do not posit a social planner who is able to trade-off consumer and producer welfare on an additive scale. Instead, while in our model producers still have a quantitative (differentiable, convex) cost function, consumer welfare is only captured via hard constraints (i.e., we must respect their indifference sets); the main role of prices is then to induce consumers to substitute peak-hour demand with non-peak demand. Several mathematical tools used by Adelman and Uçkun [2019]—such as the implicit function theorem to capture consumer response to prices—are no longer applicable in our setting, and thus our technical development is not closely related to theirs.

In another related line of work, Zhou et al. [2017] consider demand-response programs that employ price incentives, where each consumer aims to minimize their own cost function. This cost function is composed of two parts: one that reflects power consumption and remains independent of price incentives (e.g., minimizing deviation from a nominal consumption level), and another that accounts for the expenses incurred due to price incentives. Building on this framework, Zhou et al. [2019] extends the analysis to incorporate discrete decision variables and dynamically coupled devices over time, such as HVAC systems. Their approach shares similarities with ours, particularly in modeling consumer objectives as minimizing cost functions and solving a social-welfare optimiza-

tion problem (the direct method in our setup) to determine optimal pricing strategies. However, there are notable differences. In their model, the grid’s utility function is solely governed by voltage constraints, without considering the cost of supply as a function of total consumption. In this setup, and assumptions including strong convexity of consumers’ cost functions (the first component), the social welfare bi-level optimization problem can be reformulated into a convex problem, making it tractable to find optimal prices. These results, however, do not apply to our setting as the consumer cost functions are not strongly convex under our indifference-set approach—and in fact pricing mechanisms generally fail to be efficient in our model.

Meanwhile, on the side of incentive-based programs, Agrawal and Yücel [2022], Daniels and Lobel [2014], and Webb et al. [2019] have explored direct load control contracts, where utility companies manage customer loads, typically to reduce consumption as a form of demand response. Fattahi et al. [2023] formulates a stochastic dynamic program to design optimal contracts and develop approximation methods to achieve near-optimal solutions for energy consumption. They avoid explicitly referring to these contracts as demand response due to their complexity and the extended nature of the control periods. In contrast, in the pricing algorithm we evaluate in our experiments, the grid has no explicit control over users’ consumption; instead, HEMS selects optimal consumption profiles that meet users’ needs while minimizing costs. Finally, Allcott [2011b] studies the effect of “home energy reports” that compare a consumer’s energy use to that of their neighbors, and finds that such programs can meaningfully shift behavior.

2 Optimal Demand Response

We consider a model with $j = 1, \dots, d$ time periods, e.g., $d = 24$ for hourly planning over the course of a day, and with $i = 1, \dots, n$ consumers. Each consumer has certain needs that must be met—for example, maintaining indoor temperatures within acceptable bounds or ensuring that an electric vehicle (EV) is charged overnight—and they will consume electricity $q_i \in \mathbb{R}^d$ to meet these needs. The grid operator has access to a variety of energy resources, such as gas, wind and/or solar plants, that can be used to produce this energy. We assume that the renewable energy resources, such as wind and solar, exogenously produce energy $Q_0 \in \mathbb{R}^d$ at zero marginal cost; the grid operator then needs to deploy non-renewable resources to meet the remaining demand $\sum_{i=1}^n q_i - Q_0$.

The goal of a demand-response program is to shift consumer demand so that the grid can produce the needed energy more efficiently, and in particular so that it can avoid spikes in net demand for non-renewable energy. We formalize the underlying problem as follows:

Definition 1. The **indifference set** $R_i \subset \mathbb{R}^d$ of each consumer is the set of all energy consumption profiles that allow the consumer to meet their pre-specified needs.

Definition 2. The **optimal demand response** problem involves implementing acceptable energy consumption profiles for each consumer such as to optimize a grid objective. If the grid has a cost function $\sigma(Q, Q_0)$ for producing energy $Q \in \mathbb{R}^d$ given renewable production Q_0 , then the optimal demand response problem requires finding a solution to

$$\widehat{R}_n^{\text{DM}} = \min \left\{ \sigma \left(\sum_{i=1}^n q_i, Q_0 \right) : q_i \in R_i \text{ for all } i = 1, \dots, n \right\}. \quad (1)$$

We give some idealized examples of possible indifference sets below. Throughout, we assume that we are planning energy consumption over a 24 hour period starting at midnight so, e.g., q_{i1}

is the consumption in kWh of the i -th user between midnight and 1am, etc. The examples below are intentionally simple; and we emphasize that our formal results allow full flexibility in specifying these indifference sets. We will not require any specific parametrizations or functional forms for these sets; rather, we will simply assume that each consumer has a HEMS that understands their own acceptable energy consumption profiles.

Example 1. Consider a consumer who only needs to add 50 kWh of charge to an electric vehicle by 7 am. Their indifference set is then $\mathbf{R}_1 = \{q \geq 0 : \sum_{j=1}^7 q_j = 50, q_j = 0 \text{ for all } j > 7\}$.

Example 2. Consider a consumer who only needs to run their dryer between 8 and 11 AM, which requires 3 kWh over a 1 hour period. Their indifference set is then $\mathbf{R}_2 = \{q \geq 0 : \sum_{j=8}^{11} q_j = 3, \text{ where } q_j = 0 \text{ or } 3 \text{ for all } 8 \leq j \leq 11, \text{ and } q_j = 0 \text{ else}\}$.

Example 3. Consider a consumer who only wants operate an air conditioner to maintain the indoor temperature of their house within an acceptable range. Following Li et al. [2011], we model indoor temperature dynamics using the following linear formulation motivated by the heat equation,

$$T_t^{\text{in}} = T_{t-1}^{\text{in}} + \alpha(T_t^{\text{out}} - T_{t-1}^{\text{in}}) + \beta q_t, \quad (2)$$

where $\alpha \in \mathbb{R}$ captures the insulation properties of the house, and $\beta < 0$ represents the cooling efficiency power of the system. Writing $[T^{\text{min}}, T^{\text{max}}]$ for the acceptable temperature range, and T_0^{in} for the initial indoor temperature, the consumer's indifference set then becomes:

$$\mathbf{R}_3 = \left\{ q \geq 0 : T^{\text{min}} \leq \sum_{i=1}^j (1 - \alpha)^{i-j} (\beta q_i + \alpha T_i^{\text{out}}) + (1 - \alpha)^j T_0^{\text{in}} \leq T^{\text{max}} \text{ for all } 1 \leq j \leq 24 \right\}.$$

Example 4. Consider a consumer who wants to operate all 3 devices described above. Then their indifference set is $\mathbf{R}_4 = \mathbf{R}_1 \oplus \mathbf{R}_2 \oplus \mathbf{R}_3$.

Our main goal of this paper is to characterize solutions to the optimal demand response problem, and to design algorithms for achieving optimal consumption. For flexibility, we will not seek to model individual consumer devices directly; rather, we will assume throughout that we interact with consumers via a HEMS device. This assumption is in line with current practice [Beaudin and Zareipour, 2015, Zhou et al., 2016].

Definition 3. A **home energy-management system (HEMS)** serving consumer i is a device that can

1. Compute the indifference set \mathbf{R}_i in terms of the consumer's high-level preferences and device properties;
2. Communicate with the grid operator; and
3. Choose and implement a consumption profile $q_i \in \mathbf{R}_i$.

At this point, our setting is still very abstract: For example, our definitions so far, it would, in principle, allow for the HEMS to give the grid operator direct control of all consumer devices, and let the grid solve the optimization problem (1). This approach would, of course, achieve optimal demand response, but would likely not be implementable in real-world systems. A more practical alternative is to decouple decision making by the grid and by the HEMS via a price mechanism: The HEMS optimizes consumption to minimize energy costs under (potentially time-varying) prices, and the grid chooses prices such as to induce desirable consumption profiles.

Definition 4. A **price-responsive HEMS** is a HEMS as in Definition 3 that receives a price-vector $p \in \mathbb{R}^d$ from the grid, and then chooses

$$q_i := q_i(p) \in \operatorname{argmin}_q \{p \cdot q : q \in \mathbf{R}_i\}. \quad (3)$$

In a system where consumers operate price-responsive HEMS, the grid's optimal pricing problem becomes a bi-level optimization problem [Zhou et al., 2017]:

$$p^* \in \operatorname{argmin}_p \left\{ \sigma \left(\sum_{i=1}^n q_i(p), Q_0 \right) \right\}, \quad (4)$$

resulting in an objective value $\widehat{\mathbf{R}}_n^{\text{PM}}$. Note that, in the above definition, price-responsive HEMS are only responsive to variation in the price and not in the overall level of the price, i.e., $q_i(p) = q_i(\lambda p)$ for any $\lambda > 0$. This reflects our modeling assumption that demand-response programs can only shift energy consumption within the indifference set that reflects the user's pre-determined needs; they cannot induce consumers to revisit their needs. Similarly, optimal prices in (4) are scale invariant: If p^* is optimal, then λp^* is also optimal for any $\lambda > 0$. Thus, a successful demand response will only depend on the relative magnitude of prices across the day, and the overall price levels can be chosen to match revenue targets; see the discussion following Theorem 5 for more details.

We are now ready to state our main research questions: First, can a pricing mechanism as in (4) solve the optimal demand response problem (1), or will systems with pricing-based HEMS fall short of what could be achieved via direct device control by the grid? Second, if an optimal pricing mechanism exists, are there computationally efficient and practically applicable algorithms to learn the optimal prices? Overall, we will find that while price-based mechanisms may be suboptimal in finite systems, optimality gap of pricing as in (4) vanishes as the system size grows. Furthermore, optimal prices can be recovered via a simple first-order algorithm.

2.1 A Warm-up Illustration

Before attempting a general answer to these questions, we begin by examining both direct and price-based approaches to demand response in a simplified scenario where the problems (1) and (4) can be solved explicitly. We consider a two-period setting with no renewable production (i.e., with $Q_0 = 0$), and where the grid wants to minimize peak demand (and thus to use demand-response programs to shift consumer demand away from peak periods); the grid cost functions is $\sigma(Q) = \sup \{Q_j : j = 1, \dots, d\}$. Finally, we assume that each consumer has a linear indifference set

$$\mathbf{R}_i = \{q \in \mathbb{R}_+^2 : q_1/a_i + q_2/b_i = 1\}, \quad (5)$$

where $a_i, b_i > 0$ are consumer-specific parameters.

Proposition 1. *Consider the above setting with $i = 1, \dots, n$ users with indifference sets as in (5), and where the grid seeks to minimize peak-load. Then, optimal demand response as in (1) achieves an objective value*

$$\widehat{\mathbf{R}}_n^{\text{DM}} = \max_{0 \leq z \leq 1} \{L_n(z)\}, \quad L_n(z) = \sum_{i=1}^n ((1-z)b_i \mathbb{I}((1-z)b_i < za_i) + za_i \mathbb{I}((1-z)b_i \geq za_i)). \quad (6)$$

Meanwhile, optimal pricing as in (4) achieves

$$\widehat{R}_n^{\text{PM}} = \min_{0 \leq z \leq 1} \{U_n(z)\}, \quad U_n(z) = \min \{U_n^+(z), U_n^-(z)\}, \quad (7)$$

where $U_n^+(z), U_n^-(z)$ are given by

$$U_n^+(z) = \max \left\{ \sum_{i=1}^n a_i \mathbb{I}(a_i z \leq b_i(1-z)), \sum_{i=1}^n b_i \mathbb{I}(a_i z > b_i(1-z)) \right\},$$

$$U_n^-(z) = \max \left\{ \sum_{i=1}^n a_i \mathbb{I}(-a_i z \leq b_i(-1+z)), \sum_{i=1}^n b_i \mathbb{I}(-a_i z > b_i(-1+z)) \right\}.$$

Because direct optimization is guaranteed to achieve optimal demand response, we know that we must have

$$\max_{0 \leq z \leq 1} \{L_n(z)\} \leq \min_{0 \leq z \leq 1} \{U_n(z)\},$$

and furthermore, the size of the vertical gap between these functions $L_n(z)$ and $U_n(z)$ can be used to measure the sub-optimality of the pricing mechanism. To gain further insight into this gap, we simulate consumers and draw the indifference set parameters in (5) as

$$a_i, b_i \stackrel{\text{iid}}{\sim} \text{Unif}[0, 2]. \quad (8)$$

In Figure 2, we plot the resulting $L_n(z)$ and $U_n(z)$ curves for both a realization of a small system with $n = 10$ consumers and a realization of a larger system with $n = 100$ consumers.

We immediately see that, in the small system, pricing is suboptimal: Direct control achieves scaled peak demand of 0.35, while optimal pricing can only get to a scaled peak demand of 0.41; in other words, the grid cost with optimal pricing is 17% higher with pricing than with direct control. However, this the optimality gap of pricing essentially vanishes as we scale the system up to $n = 100$ customers; visually we already see no gap in Figure 2 at this scale. Below, we will prove that this finding was no accident—and that, while potentially suboptimal in small systems, pricing mechanisms are quasi-optimal in large systems under considerable generality.

3 Mean-field Optimality of Dynamic Pricing

To present our main result on large-sample optimality of pricing mechanisms for demand response, we first need to introduce some notation. Let \mathfrak{C}_d denote the space of all non-empty compact subsets of \mathbb{R}^d . For two sets $C_1, C_2 \in \mathfrak{C}_d$, we write their Minkowski sum as

$$C_1 \oplus C_2 = \{c_1 + c_2 : c_1 \in C_1, c_2 \in C_2\}.$$

For any non-empty subset C of \mathbb{R}^d , we define its support function as

$$\delta(s; C) = \sup \{c \cdot s : c \in C\}. \quad (9)$$

We measure set similarity using the Hausdorff distance

$$d_{\text{H}}(C_1, C_2) = \inf \{\varepsilon > 0 : C_1 \in C_2 \oplus B_\varepsilon(0), C_2 \in C_1 \oplus B_\varepsilon(0)\},$$

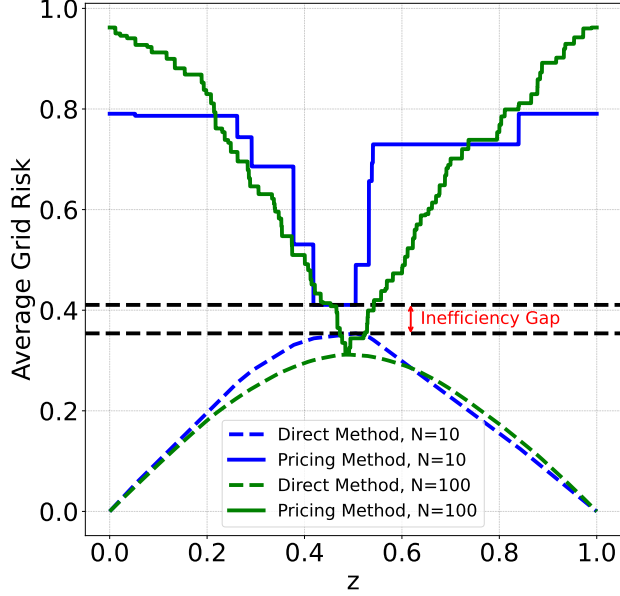


Figure 2: Peak demand achieved via the direct control and pricing mechanisms in the setting of Proposition 1, in both a small system with $n = 10$ consumers and a larger system with $n = 100$ consumers. For direct control, we plot $n^{-1}L_n(z)$ (and the scaled optimal objective value is the maximum of this function), while for pricing we plot $n^{-1}U_n(z)$ (and the scaled optimal objective value is the minimum of this function).

where $B_r(x) \subset \mathbb{R}^d$ denotes the d -dimensional Euclidean ball of radius r centered at x . Recall we have assumed that each user has an indifference set $\mathbf{R} \subset \mathbb{R}^d$; for our analysis, we will take these indifference sets to be random, and we construct random sets $\mathbf{R} \in \mathfrak{C}_d$ as follows. Given a probability space (Ω, \mathcal{F}, P) , we say that a multifunction $R : \Omega \rightrightarrows \mathfrak{C}_d$ is measurable if, for all open sets $O \subset \mathbb{R}^d$

$$R^{-1}(O) = \{\omega \in \Omega : R(\omega) \cap O \neq \emptyset\}$$

is measurable [Rockafellar and Wets, 2009, Chapter 14]. We say that a random set is measurable if $\mathbf{R} = R(\omega)$ for a measurable multifunction.³ We further define a selection of a random set \mathbf{R} as any random variable $X \in \mathbb{R}^d$ with [Vitale, 1990]

$$\mathbb{P}(X \in \mathbf{R}) = 1, \quad \mathbb{E}[\|X\|] < \infty, \quad (10)$$

i.e., a random variable that always chooses an element from the random set; and define the expected value of a random set as

$$\mathbb{E}[\mathbf{R}] = \{q = \mathbb{E}[X] : X \text{ is a selection of } \mathbf{R}\}, \quad (11)$$

while noting that if $\mathbb{E}[\|\mathbf{R}\|] < +\infty$, then $\mathbb{E}[\mathbf{R}]$ is non-empty and $\mathbb{E}[\mathbf{R}] \in \mathfrak{C}_d$ [Aumann, 1965]. This notion of a random set results in the following strong law of large numbers: If $\mathbb{E}[\|\mathbf{R}\|] < \infty$, then [Artstein and Vitale, 1975]

$$\lim_{n \rightarrow \infty} d_H \left(\frac{1}{n} \bigoplus_{i=1}^n \mathbf{R}_i, \mathbb{E}[\text{conv}(\mathbf{R})] \right) =_{a.s.} 0, \quad (12)$$

³Some papers cited below use different definitions of measurability for random sets; see Bellay [1986] for results on the equivalence of these definitions.

where conv denote the convex hull operation.⁴ We are now ready to state our main assumptions.

Assumption 1. The user indifference sets are independent and identically from a distribution over \mathcal{C}_d ; in more detail, we assume that there is a non-atomic probability space (Ω, \mathcal{F}, P) and a measurable multifunction $R : \Omega \rightrightarrows \mathcal{C}_d$ such that $\mathbf{R} = R(\omega)$. Furthermore, we assume that $\mathbb{E}[\|\mathbf{R}\|] < +\infty$.

Assumption 2. The grid costs can be represented in terms of a convex function $\rho : \mathbb{R}^d \rightarrow \mathbb{R}$ of net demand, i.e., $\sigma(Q, Q_0) = \rho(Q - Q_0)$. Furthermore, $\rho(\cdot)$ is order-one positively homogeneous, i.e., for every $\alpha \geq 0$ and $q \in \mathbb{R}^d$ we have that $\rho(\alpha q) = \alpha \rho(q)$.

We note that the net-demand cost function $\rho(\cdot)$ can flexibly capture many types of costs. For example, cost functions that satisfy this assumption include $\rho(q) = \|q\|_\infty$ which measures peak demand; $\rho(q) = \sum_{j=1}^d |q_j|$ which measures total demand; $\rho(p) = \|q\|_\kappa = (\sum_{j=1}^d q_j^\kappa)^{1/\kappa}$ for $\kappa > 1$ which makes a compromise between these two; or $\rho(p) = \|q\|_\kappa + \lambda \sum_{j=1}^{d-1} |q_{j+1} - q_j|$ with $\lambda > 0$ which adds an extra penalty for fast ramp-ups or ramp-downs in demand. We now state some technical results that highlight key consequences of these assumptions. First, under our setting, set-expectation commutes with the user cost function in the following sense:

Lemma 2. Write the user- i cost function from solving (4) as

$$h(p; \mathbf{R}_i) = \min \{q \cdot p : q \in \mathbf{R}_i\}; \quad (13)$$

and, under Assumption 1, let $H(p) = h(p; \mathbb{E}[\mathbf{R}_i])$. Then, for any $p \in \mathbb{R}^d$ we also have $H(p) = \mathbb{E}[h(p; \mathbf{R}_i)]$.

Proof. The user cost function can also be written as a support function, i.e., $h(p; \mathbf{R}_i) = -\delta(-p; \mathbf{R}_i)$; thus, proving our desired result is equivalent to showing that

$$\mathbb{E}[\delta(p; \mathbf{R}_i)] = \delta(p; \mathbb{E}[\mathbf{R}_i])$$

for all p in \mathbb{R}^d . We now note 3 well-known facts in convex analysis: (1) For any random set \mathbf{C} that is almost surely convex, we have [Artstein, 1974]

$$\mathbb{E}[\delta(u; \mathbf{C})] = \delta(u; \mathbb{E}[\mathbf{C}]) \text{ for all } u \in \mathbb{R}^d;$$

(2) Whenever \mathbf{R}_i has a non-atomic distribution, we have $\mathbb{E}[\text{conv}(\mathbf{R}_i)] = \mathbb{E}[\mathbf{R}_i]$ [Aumann, 1965, Artstein, 1974]; and (3) the support function of a set and its convex hull are equal, i.e., $\delta(\cdot; \mathbf{R}) = \delta(\cdot; \text{conv}(\mathbf{R}))$. It then follows that

$$\mathbb{E}[\delta(p; \mathbf{R}_i)] \stackrel{(3)}{=} \mathbb{E}[\delta(p; \text{conv}(\mathbf{R}_i))] \stackrel{(1)}{=} \delta(p; \mathbb{E}[\text{conv}(\mathbf{R}_i)]) \stackrel{(2)}{=} \delta(p; \mathbb{E}[\mathbf{R}_i]),$$

as claimed. \square

Second, under Assumption 2, there exists a compact convex set $\mathcal{P} \subset \mathbb{R}^d$ such that $\rho(\cdot)$ is its support function [e.g., Artstein-Avidan et al., 2015, Claim A.2.24]:⁵

$$\rho(q) = \delta(q; \mathcal{P}), \quad \mathcal{P} = \left\{ z \in \mathbb{R}^d : z \cdot q \leq \rho(q), \quad \forall q \in \mathbb{R}^d \right\}. \quad (14)$$

Given these technical preliminaries, we are now ready to state the first characterization result.

⁴Note that since $\text{conv}(\mathcal{C}_d)$ is a closed subset of \mathcal{C}_d and conv is a continuous mapping with respect to the Hausdorff distance in a finite-dimensional space, $\text{conv}(\mathbf{R})$ is measurable, and its expectation is well-defined.

⁵See Lemma 9 in the Appendix for a self-contained proof of this claim.

Theorem 3. Under Assumptions 1 and 2, suppose we have a sequence of systems with renewable production scaling with system size, $\lim_{n \rightarrow \infty} Q_0/n =_{a.s.} q_0$. Then,

1. The scaled cost of the direct control mechanism converges almost surely,

$$\lim_{n \rightarrow \infty} \frac{1}{n} \widehat{\mathbf{R}}_n^{\text{DM}} = \mathbf{R}^{\text{DM}} := \max \{H(z) - z \cdot q_0 : z \in \mathcal{P}\}, \quad (15)$$

where \mathcal{P} is given in (14), and $H(\cdot)$ is as in Lemma 2.

2. For any price p , if the mean-field cost function $H(\cdot)$ is differentiable at p , then the scaled grid cost from using prices p converges almost surely,

$$\lim_{n \rightarrow \infty} \frac{1}{n} \sigma \left(\sum_{i=1}^n q_i(p), Q_0 \right) = \rho(\nabla H(p) - q_0). \quad (16)$$

Proof. We start with part 1. Let

$$\widehat{\mathbf{R}}_n = \frac{1}{n} \bigoplus_{i=1}^n \mathbf{R}_i$$

denote the Minkowski average of the user indifference sets. By Assumption 2,

$$\begin{aligned} \frac{1}{n} \widehat{\mathbf{R}}_n^{\text{DM}} &= \min \left\{ \frac{1}{n} \sigma \left(\sum_{i=1}^n q_i, Q_0 \right) : q_i \in \mathbf{R}_i \text{ for all } 1 \leq i \leq n \right\} \\ &= \min \left\{ \rho \left(\frac{1}{n} \sum_{i=1}^n q_i - Q_0 \right) : q_i \in \mathbf{R}_i \text{ for all } 1 \leq i \leq n \right\} \\ &= \min \left\{ \rho(q - Q_0/n) : q \in \widehat{\mathbf{R}}_n \right\}. \end{aligned} \quad (17)$$

Thus, by the strong law of large numbers (12), the almost sure convergence of Q_0/n and Lipschitz-continuity of ρ , we have

$$\lim_{n \rightarrow \infty} \frac{1}{n} \widehat{\mathbf{R}}_n^{\text{DM}} =_{a.s.} \min \{ \rho(q - q_0) : q \in \mathbb{E}[\mathbf{R}] \}. \quad (18)$$

Now, by the characterization of $\rho(\cdot)$ given in (14), we have

$$\min_{q \in \mathbb{E}[\mathbf{R}]} \{ \rho(q - q_0) \} = \min_{q \in \mathbb{E}[\mathbf{R}]} \left\{ \max_{z \in \mathcal{P}} \{ z \cdot (q - q_0) \} \right\}.$$

Furthermore, $\mathbb{E}[\mathbf{R}]$ is convex as argued in the proof of Lemma 2 and compact because $\mathbb{E}[\|\mathbf{R}\|] < \infty$, so by the minimax theorem

$$\min_{q \in \mathbb{E}[\mathbf{R}]} \left\{ \max_{z \in \mathcal{P}} \{ z \cdot (q - q_0) \} \right\} = \max_{z \in \mathcal{P}} \left\{ \min_{q \in \mathbb{E}[\mathbf{R}]} \{ z \cdot (q - q_0) \} \right\} = \max_{z \in \mathcal{P}} \{ H(z) - z \cdot q_0 \},$$

which establishes (15).

Moving to part 2, we start by noting that—in our model—the user energy consumption $q_i(p)$ is a subgradient of the user cost $h(p; \mathbf{R}_i)$, i.e., $q_i(p) \in \partial h(p; \mathbf{R}_i)$. To verify this claim, we note that

$h(p; \mathbf{R})$ is concave because it is a point minimization of concave functions $p \cdot q$, and $h(p; \mathbf{R}_i) = p \cdot q_i(p)$. Now, for any p' ,

$$q_i(p) \cdot p' = q_i(p) \cdot p + (p' - p) \cdot q_i(p) = h(p; \mathbf{R}_i) + (p' - p) \cdot q_i(p).$$

Writing $q_i(p')$ for optimal consumption under p' , we must have $p' \cdot q_i(p') \leq p' \cdot q_i(p)$, and so

$$h(p'; \mathbf{R}_i) = p' \cdot q_i(p') \leq p' \cdot q_i(p) = h(p; \mathbf{R}_i) + (p' - p) \cdot q_i(p). \quad (19)$$

Finally, $q_i(p) \in \partial h(p; \mathbf{R}_i)$ because the above holds for any $p' \in \mathbb{R}^d$.

Next, because $h(p; \mathbf{R}_i)$ is concave, its subgradient $\partial h(p; \mathbf{R})$ is a measurable random set [Shapiro et al., 2021, Remark 30]. Furthermore, because $\mathbb{E}[h(p; \mathbf{R}_i)] = H(p)$ by Lemma 2, our assumption that $H(\cdot)$ is differentiable at p implies that $h(\cdot; \mathbf{R}_i)$ is almost surely differentiable at p and $\mathbb{E}[\nabla h(p; \mathbf{R}_i)] = \nabla H(p)$ [Shapiro et al., 2021, Theorem 7.46]. Finally, because $q_i(p) \in \partial h(p; \mathbf{R}_i)$ as shown above, almost sure differentiability of $h(p; \mathbf{R}_i)$ implies that $q_i(p) = \nabla h(p; \mathbf{R}_i)$ almost surely, that $\mathbb{E}[q_i(p)] = \nabla H(p)$. Thus, by the strong law of large numbers,

$$\lim_{n \rightarrow \infty} \frac{1}{n} \sum_{i=1}^n q_i(p) =_{a.s.} \nabla H(p), \quad (20)$$

and (16) follows from Assumption 2, by invoking homogeneity and Lipschitz-continuity of $\rho(\cdot)$ (see Lemma 9 in the appendix). \square

The above result gives the scaled costs for both the direct and price-based mechanisms; it now remains to show that (15) and the minimizer of (16) over p match. The function $\rho(\nabla H(p) - q_0)$ is not necessarily convex in p because it depends on p through the differential of H ; thus, classic duality theory for convex functions does not apply here. The following result nonetheless establishes optimality of the price-based mechanism under a differentiability condition.

Assumption 3. We assume that $h(z, \mathbf{R}_i)$ as defined in (13) is almost surely differentiable at any point

$$z^* \in \operatorname{argmax} \{H(z) - z \cdot q_0 : z \in \mathcal{P}\}. \quad (21)$$

Theorem 4. Under the conditions of Theorem 3, suppose furthermore that Assumption 3 holds. Then $H(z)$ is differentiable at z^* , and we have

$$\rho(\nabla H(z^*) - q_0) = H(z^*) - z^* \cdot q_0. \quad (22)$$

Furthermore, using prices $p^* = \lambda z^*$ with any $\lambda > 0$ asymptotically solves the optimal demand response problem.

Proof. As noted above, $H(\cdot)$ and $h(\cdot, \mathbf{R})$ are both concave; thus, for any $z \in \mathbb{R}^d$, $H(\cdot)$ is differentiable at z if and only if $h(\cdot, \mathbf{R})$ is differentiable at z almost surely [Shapiro et al., 2021, Theorem 7.46]. Assumption 3 thus implies that $H(\cdot)$ is differentiable for all $z^* \in \operatorname{argmax} \{H(z) - z \cdot q_0 : z \in \mathcal{P}\}$. Given that z^* is a maximizer of $H(z) - z \cdot q_0$ over \mathcal{P} , the first-order optimality condition then implies that

$$\max \{(z - z^*) \cdot (\nabla H(z^*) - q_0) : z \in \mathcal{P}\} = 0.$$

Furthermore, by Euler's homogeneous function theorem $z^* \cdot \nabla H(z^*) = H(z^*)$, and so

$$\max \{z \cdot (\nabla H(z^*) - q_0) - (H(z^*) - z^* \cdot q_0) : z \in \mathcal{P}\} = 0.$$

Finally, given the definition of \mathcal{P} in (14), this implies that

$$\rho(\nabla H(z^*) - q_0) - (H(z^*) - z^* \cdot q_0) = 0.$$

By comparing this expression with (15) and (16) we see that the asymptotic costs of the direct control method and pricing with z^* match (recall that z^* is a maximizer of $H(p) - p \cdot q_0$), and thus pricing with z^* achieves optimal demand response in the large-sample limit. Finally, as discussed following Definition 4, users with a price-responsive HEMS are unresponsive to scaling prices by a positive scalar. Thus, pricing with $p^* = \lambda z^*$ for any $\lambda > 0$ results in the same consumption profiles—and also solves the optimal demand-response problem in large samples. \square

Theorem 4 above showed that, under considerable generality, pricing with prices of the form $p^* = \lambda z^*$ with $\lambda > 0$ and z^* as in (21) solves the demand-response problem. This abstract result highlights the promise of the pricing mechanism, but also raise some immediate practical questions such as

1. Are energy markets with dynamic prices p^* stable?
2. How should we pick the scale parameter $\lambda > 0$? Price-responsive HEMS as in Definition 4 may be unresponsive to price scale; however, consumers, grid operators and regulators will of course care about the overall level of prices.
3. When can we guarantee that optimal prices are positive? Negative prices are known to sometimes arise in practice when renewable production overwhelms demand; however, we may believe that healthy demand-response mechanisms would avoid negative prices.

This section gives some (largely reassuring) answers to these questions.

We start with a positive answer to the first question, and verify that our proposed pricing method results in stable consumer behavior. Qualitatively, the reason this holds is our Assumption 3 that $h(p, \mathbf{R}_i)$ is almost surely differentiable at p^* . This assumption reflects a requirement that consumers are price-responsive at p^* , thus enabling us to use prices to shift demand in a predictable way.

Theorem 5. *Let z^* be an optimal price under the conditions of Theorem 4. Then:*

1. *For each customer, with probability one, there exists a unique optimal energy consumption profile that optimizes the consumer objective under the price z^* , i.e., for consumer i the following set is almost surely a singleton:*

$$\Theta_i(z^*) = \{q \in \mathbf{R}_i : q_i \cdot z^* = h(z^*; \mathbf{R}_i)\}. \quad (23)$$

2. *The average consumption profile of consumers under the optimal price z^* is unique, i.e., $\mathbb{E}[\Theta_i(z^*)]$ is a singleton, and furthermore*

$$\mathbb{E}[\Theta_i(z^*)] = \Theta(z^*), \quad \Theta(z^*) = \{q \in \mathbb{E}[\mathbf{R}], q \cdot z^* = h(z^*; \mathbb{E}[\mathbf{R}])\}. \quad (24)$$

We denote this average consumption profile by $\bar{q}(z^)$, i.e., $\Theta(z^*) = \{\bar{q}(z^*)\}$.*

Next, given that our model is agnostic to the scale parameter λ , this parameter can simply be chosen to match a target grid revenue. Given Theorem 5, we know that average per-consumer grid revenue from net demand with prices p^* is stable, and equal to $U(p^*) = (\bar{q}(p^*) - q_0) \cdot p^*$. Thus, given a candidate price schedule z^* (e.g., as in (21)), and a target per-consumer revenue C , and provided that $U(z^*) > 0$, we can achieve optimal demand-response at the target per-user revenue, i.e., with $U(p^*) = C$, by using with prices⁶

$$p^* = C z^* / U(z^*). \quad (25)$$

The following result establishes conditions under which $U(z^*) > 0$, and so this scaling can be applied.

Corollary 6. *Under the conditions of Theorem 4, suppose furthermore that for non-negative grid cost function $\rho(\cdot)$ we have $\rho(x) = 0$ if and only if $x = 0$, and that $q_0 \notin \mathbb{E}[\mathbf{R}_i]$. Then, for any z^* as in (21) we have that $U(z^*) = (\bar{q}(z^*) - q_0) \cdot z^* > 0$.*

Finally, we verify below that prices are in fact positive, as expected, whenever the following two conditions stated in the next assumption are satisfied.

Assumption 4. We assume that the average indifference set stochastically dominates available renewables, i.e., $q \geq q_0$ componentwise for all $q \in \mathbb{E}[\mathbf{R}_i]$.

Corollary 7. *Under conditions of Theorem 4 and Assumption 4, Suppose furthermore that the grid cost function $\rho(\cdot)$ satisfies a monotonicity property⁷ whereby for each pair $q, r \in \mathbb{R}^d$ if either $0 \leq r_j \leq q_j$ or $q_j \leq r_j = 0$ for each $j = 1, \dots, d$, then also $\rho(r) \leq \rho(q)$. Then the optimal prices p^* as described in the statement of Theorem 4 satisfy $p^* \geq 0$.*

4 A First-order Algorithm for Optimal Pricing

In the previous section, we found that dynamic pricing is mean-field optimal for demand response under our indifference-set model, and any prices p^* of the form

$$p^* = \lambda z^*, \quad z^* \in \arg \max_{z \in \mathcal{P}} \{H(z) - z \cdot q_0\}, \quad H(z) = \mathbb{E}[h(z; \mathbf{R}_i)], \quad (26)$$

for any $\lambda > 0$, where $h(z; \mathbf{R}_i)$ is the minimal spending for a consumer with indifference set \mathbf{R}_i and q_0 is the scaled renewable production. In order to make use of the result in practice, we need a way of learning prices from data. One natural way of doing so is via empirical maximization with

$$\hat{p} = \lambda \hat{z}, \quad \hat{z} \in \arg \max_{z \in \mathcal{P}} \left\{ \hat{H}(z) - z \cdot q_0 \right\}, \quad \hat{H}(z) = \frac{1}{n} \sum_{i=1}^n h(z; \mathbf{R}_i), \quad (27)$$

where again $\lambda > 0$ is planner-chosen scale parameter. Below, we verify that such empirical maximization achieves optimal demand response in large samples.

⁶Under the proposed prices, revenue is $(q(p^*) - q_0) \cdot p^* = (q(z^*) - q_0) \cdot p^* = (q(z^*) - q_0) \cdot z^* C / ((q(z^*) - q_0) \cdot z^*) = C$.

⁷This monotonicity property is satisfied, e.g., for grid cost functions given by the ℓ_p norm of net demand $\|q - q_0\|_{\ell_p}$, or the non-negative component of net demand $\|\max(q - q_0, 0)\|_{\ell_p}$.

For any $z \in \mathcal{P}$ at which $H(\cdot)$ is differentiable, the mean-field suboptimality gap (i.e., then mean-field gap between deploying this price and the direct method grid risk value) following (15) and $\bar{q}(z)$ as in Theorem 5 can be characterized as

$$\Delta(z) = z \cdot (\bar{q}(z) - q_0) - \mathbf{R}^{\text{DM}}. \quad (28)$$

Recall that when $H(\cdot)$ is differentiable at z , the average consumption $\bar{q}(z)$ is the unique solution to $\min_{q \in \mathbb{E}[\mathbf{R}]} z \cdot (q - q_0)$ (see proof of Theorem 5). With this notation, Theorem 4 implies that for z^* as defined in (26), we have $\Delta(z^*) = 0$.

Theorem 8. *Under Assumptions 1 and 2, let \hat{z}_n be any sequence of prices satisfying (27) for n number of consumers. Then*

$$\lim_{n \rightarrow \infty} \Delta(\hat{z}_n) =_{a.s.} 0, \quad (29)$$

i.e., pricing with \hat{z}_n is asymptotically optimal.

The next question is then how to efficiently maximize the function $\hat{H}(z)$. At face value, the problem (27) looks like a zero-th order optimization problem: We seek to maximize a random function by taking draws at different parameter values. In general, zero-th order problems are solvable but not particularly well-behaved. In the best case scenario where we can noiselessly query the same unit multiple times, the error bound of zero-th order optimization are a factor \sqrt{d} worse than what could typically be achieved via 1-st order methods with access to gradients [Duchi et al., 2015].⁸ In addition, the situation gets much worse if there's any noise when the grid queries each HEMS to get $h(z, \mathbf{R}_i)$ (or if it's only possible to query each HEMS once); in this case, zero-th order optimization falls short of 1-st order behavior even in terms of its rate of convergence [Shamir, 2013].

Luckily, however, the proof of Theorem 3 reveals that our setting affords us with natural estimates of the gradient of the objective in (27). Since $\hat{H}_n(\cdot)$ is a concave function, by an application of Alexandrov's theorem we know that for almost every $z \in \mathcal{P}$ we have that $\hat{H}_n(z)$ is differentiable at z . In addition, given the formulation (3), it can be observed that $q_i(z)$ is a sub-gradient of $h(z; \mathbf{R}_i)$ (see arguments before (19) for more details). Putting these two results together, we realize that for almost every $z \in \mathcal{P}$, $\hat{H}_n(\cdot)$ is differentiable with derivative

$$\nabla \hat{H}_n(z) = \frac{1}{n} \sum_{i=1}^n q_i(z). \quad (30)$$

In other words, we can evaluate the gradient of our objective simply by observing the average consumption choice of each consumer at the current proposed prices.

The upshot is that we can compute system-level welfare gradients from data collected in equilibrium and thus, as argued in Wager and Xu [2021], can efficiently optimize the system using familiar 1st-order optimization methods (all while inheriting their fast convergence properties). Specifically, one can proceed via variants of the following simple meta-algorithm. Given a current candidate price schedule $z_k \in \mathbb{R}^d$:

- Send a (potentially scaled)⁹ price $p_k = \lambda z_k$ with $\lambda > 0$ to some set of HEMS \mathcal{N}_k .

⁸These methods proceed by effectively taking numerical gradients by evaluating $h(z, \mathbf{R}_i)$, $h(z', \mathbf{R}_i)$ for nearby values of z, z' .

⁹Prices could be scaled, e.g., using (25). Recall that, under our indifference-set model, consumer consumption is invariant to scaling prices by a constant positive factor.

- Observe the average consumption $\bar{q}_k = \frac{1}{|\mathcal{N}_k|} \sum_{i \in \mathcal{N}_k} q_i(p_k)$.
- Form a gradient $g_k = \bar{q}_k - q_0$, and use it to update z_k .

There is a huge number of available 1-st order algorithms that could be used here. For example, one could use standard gradient descent algorithms that repeatedly query all consumers (i.e., set $\mathcal{N}_k = \{1, \dots, n\}$), or stochastic gradient descent algorithms that learn by sequentially going through the sample and only querying each customer once (i.e., with $\mathcal{N}_k = \{k\}$).

Remark 1. For a given price p , the consumption profiles $q_i(p)$ can be determined in two ways—resulting in two very different ways of running the above algorithm in practice. The first method is through actual experimentation, where users are exposed to the price p and their consumption profiles are observed after d periods. This approach can be time-consuming as it requires direct experimentation to identify the optimal price. The second method involves a communication system between the grid operator and smart management systems. In this approach, the grid operator briefly communicates a set of prices and queries users for their selected consumption profiles. The optimal price is then chosen based on the responses from users. This method can be significantly more efficient but requires more advanced Home Energy Management Systems (HEMS) that can communicate with the grid operator.

5 Case Study: Pre-cooling in Phoenix, Arizona

In this section, we examine a sample grid of households equipped with Home Energy Management Systems (HEMS) on a summer day. To simplify the analysis, we suppose that household electricity usage is solely for cooling. In this setting, homeowners input a desired range of indoor temperatures into their energy management systems, and then HEMS calculates a power trajectory based on the outside temperature, the house’s thermal properties, user’s preferences, and the electricity price.

For the outside temperature, we use the average hourly temperature data¹⁰ of Phoenix, Arizona in July 2023. We suppose that summer days in Phoenix are relatively consistent, using data from $n = 31$ days to get the sample mean $\hat{\mu}_d^{\text{temp}}$ and the sample covariance matrix $\hat{\Sigma}_d^{\text{temp}}$ for $d = 24$ hours. In the next step, we follow the indoor temperature dynamics given as (2) in Example 3. In our model, we assume that the outside temperature is the same for all households, and that each house has a fixed preference to maintain its inside temperature within the interval $[20, 25]$ degrees, with an initial temperature of $T_0^{\text{in}} = 24$ degrees. Following the temperature dynamics (2), we suppose heterogeneity across users for thermal parameters α_i and β_i , and we let

$$\begin{aligned} \alpha_i &\stackrel{\text{iid}}{\sim} \text{Unif}(0.05, 0.08), \\ \beta_i &\stackrel{\text{iid}}{\sim} \text{Unif}(-0.35, -0.25). \end{aligned}$$

We next use Arizona’s hourly renewable energy data¹¹ for solar in July 2023 to obtain the sample mean $\hat{\mu}_d^{\text{renewable}}$ and the sample covariance matrix $\hat{\Sigma}_d^{\text{renewable}}$ for available renewable.

We consider the following grid cost function parametrized by $s \geq 1$:

$$\sigma_s(Q; Q_0) = \|\max(Q - Q_0, 0)\|_{\ell_s}. \quad (31)$$

¹⁰<https://www.visualcrossing.com/weather/weather-data-services>

¹¹<https://www.eia.gov/opendata/browser/electricity/rto>

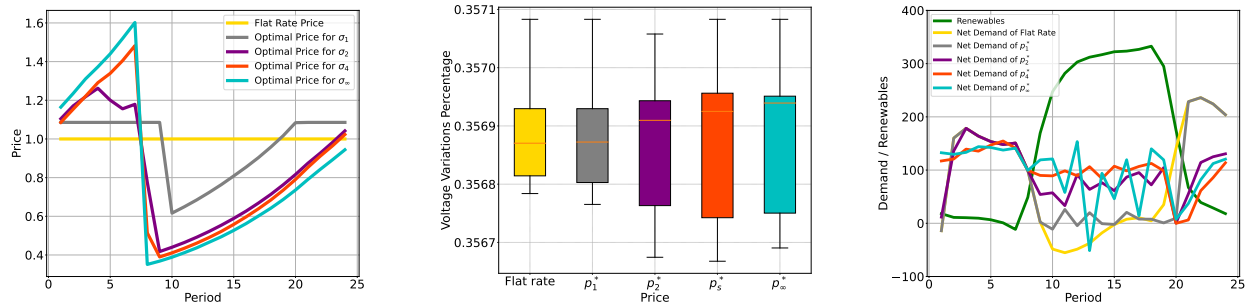
This cost function only takes into account *positive* net demand values, which require the operation of fuel-based power plants to meet the additional demand.

We first focus on the population-level (average values) quantities of outside temperature and the amount of available renewable to derive optimal dynamic price signals. Specifically, we consider the outside temperature $\hat{\mu}_d^{\text{temp}}$ and the available renewable $\hat{\mu}_d^{\text{renewable}}$ for $N = 80$ users, and we compute the optimal price p_s^* for various grid cost functions σ_s using the Frank-Wolfe method for $40k$ iterations. To obtain prices that are periodic over 24 hours—ensuring that the price values for period 1 and period 24 are close in value—we consider a problem horizon of 72 hours. In this approach, the amounts of renewable and outside temperatures are replicated three times, creating a 72-hour period. We then solve the optimization problem over this 72-hour period and report the price values for the middle 24 hours as the final obtained prices. Figure 3a shows the optimal prices normalized by revenue for $s = 1, 2, 4$, and $+\infty$. Here, we set the flat-rate pricing to be $p_0 = \mathbf{1}_d$ (all ones), and then scale all p_s^* values such that the revenue under each pricing mechanism equals that of the flat-rate pricing.

We next use the OpenDSSDirect¹² package to simulate the energy grid and solve the power flow equations, considering both active and reactive power. We suppose that HVAC system power factors are drawn i.i.d. from $\text{Unif}(0.8, 0.95)$, having available active power for each household, this would allow us to compute the reactive power as well. Each household cooling system is connected to buses with a nominal voltage of 120 volts. After solving the power flow equation for this grid, we computed the voltage variations at each period. Figure 3b shows the boxplots of the percentage variation in voltage (averaged across users) over d periods under different pricing schemes. It is evident that the overall voltage variations of devices remain within a 0.36% deviation from the nominal value at the connected buses, demonstrating the system’s stability under varying loads and dynamic pricing

For obtained prices p_s^* , we follow the HEMS response function (3) to obtain users consumption profiles. We first compute the total demand and inside temperatures in response to the price signal p_s^* for $s = 1, 2, 4$, and $+\infty$. The results are shown in Figures 3c and 3d respectively for net demand and inside temperatures. Under dynamic pricing, the average indoor temperatures exhibit a pre-cooling phase before reaching the high-demand periods, resulting in a different demand curve. In addition, a detailed view of temperature profiles of all users is exhibited in Figure 3e. For $\sigma_1, \sigma_2, \sigma_4$, and σ_∞ the total grid cost function under flat-rate pricing is respectively 2147.56, 619.29, 347.21, and 236.12, whereas when the optimal dynamic prices p_s^* are deployed, the obtained total grid cost values are respectively 2041.93, 515.96, 250.88, and 153.52. This implies approximately 4.9%, 16.7%, 27.7%, and 35.0% cost savings, respectively.

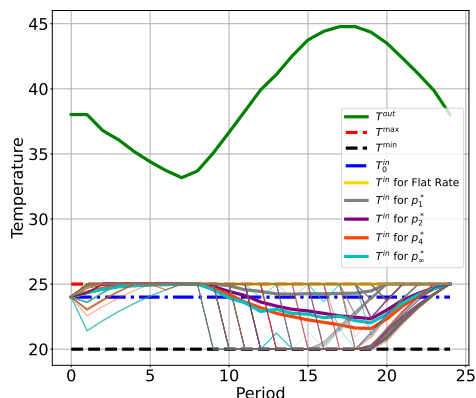
¹²<https://pypi.org/project/openssdirect.py/>



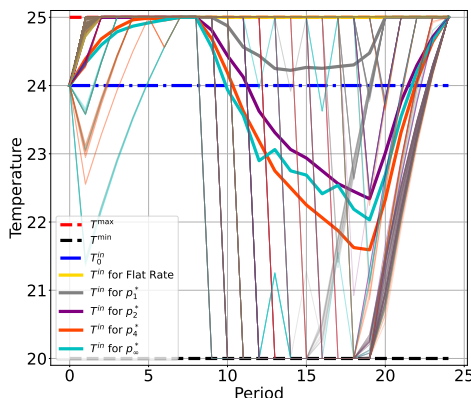
(a) Values of optimal p_s^* normalized by revenue

(b) Average voltage variations of different pricing signals

(c) Demand curves of price p_s^* and flat-rate pricing



(d) Inside temperatures and averages for p_s^*



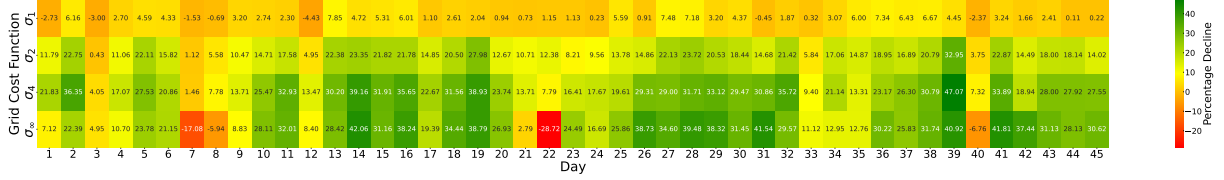
(e) Detailed inside temperatures and averages

Figure 3: Results of numerical experiments evaluating the performance of dynamic pricing. Figure 3a shows the optimal price signal p_s^* obtained using the Frank-Wolfe Algorithm for various values of the cost function $\sigma_s(\cdot)$. Figure 3b shows voltage variations for d periods across different pricing mechanisms. Figures 3c and 3d display the demand curves and inside temperature profiles under p_s^* and flat-rate pricing, respectively. Figure 3e provides a detailed (zoomed-in) view of Figure 3d. Overall, deploying the dynamic pricing p_s^* instead of flat-rate pricing results in cost savings of approximately 4.9%, 16.7%, 27.7%, and 35.0% for the grid cost functions σ_1 , σ_2 , σ_4 , and σ_∞ , respectively.

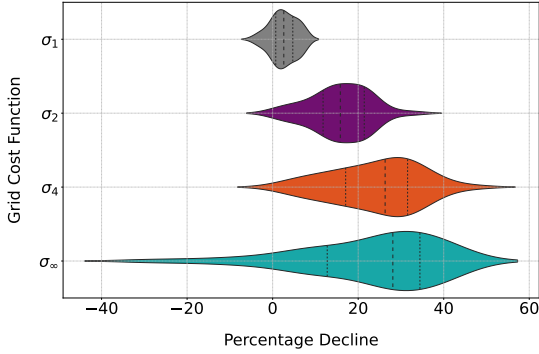
In the next experiment, we evaluate the performance of dynamic prices p_s^* when applied to different days. The objective is to examine how well the optimal price values, determined based on *mean* outside temperatures and renewable energy availability, perform on subsequent days and their effectiveness in reducing specific grid cost functions. Notably, certain days may be colder or hotter, and we aim to assess the robustness of these pricing schemes. To this end, we consider 45 *summer* days for the aforementioned 80 users, where, for each day, the outside temperature for each user is sampled from

$$T_i^{\text{out}} \stackrel{\text{iid}}{\sim} \mathcal{N}(\hat{\mu}_d^{\text{temp}}, \hat{\Sigma}_d^{\text{temp}}). \quad (32)$$

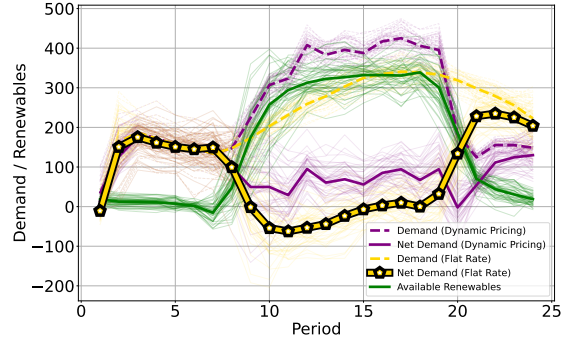
In addition, we keep the physical thermal properties of the houses, α and β , unchanged. Each day, we conduct four experiments, observing users' HEMS responses to four pricing signals: p_1^* , p_2^* , p_4^* , and p_∞^* . Our goal is to assess the effectiveness of p_s^* in reducing the grid cost function $\sigma_s(\cdot)$



(a) Daily percentage decline in grid cost function σ_s when deploying p_s^* compared to flat-rate pricing



(b) Violin plots of percentage decline in grid cost σ_s when using p_s^* compared to flat-rate pricing over 45 days

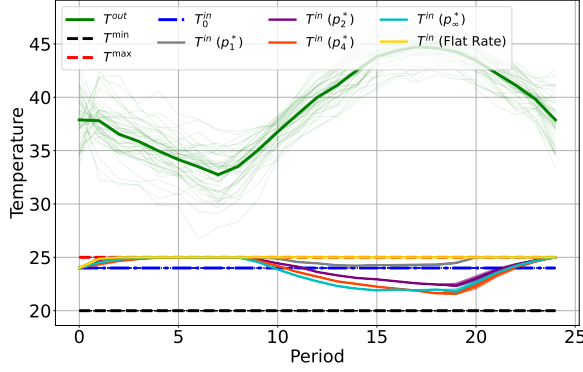


(c) Aggregated user demand and available renewables under p_s^* and flat-rate pricing for 45 days

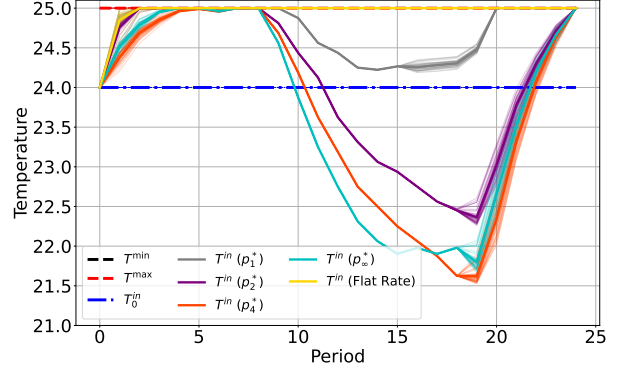
Figure 4: Comparison of grid cost, temperature dynamics, and demand profiles under optimal pricing p_s^* and flat-rate pricing over 45 days.

compared to flat-rate pricing. The exact percentage reductions in cost values compared to flat-rate pricing, calculated across all days and for various grid cost functions, are presented in Figure 4a. In addition, a summary of these results is shown in Figure 4b, where violin plots illustrate the outcomes for four values of $s = 1, 2, 4$, and $+\infty$ over 45 days. It can be observed that even with fluctuations in outside temperature, the previously computed prices are effective in reducing the grid cost function. This effect becomes more pronounced as s increases, although with greater variation. We further demonstrate the total demand curves under p_s^* and flat-rate pricing for all 45 days in Figure 4c. It is evident that the duck-shaped net-demand curve under flat-rate pricing is effectively flattened under dynamic pricing.

Finally, we compute the temperature profiles under p_s^* for various values of s and for flat-rate pricing across all 45 days, with the results displayed in Figures 5a. To better illustrate the variation among different days, we separately plot the inside temperature dynamics in Figure 5b.



(a) Outside, min/max, and inside temperature for users under p_s^* and flat-rate pricing over 45 days along with their average values



(b) Detailed view of users' indoor temperature dynamics under p_s^* and flat-rate pricing over a 45-day period, including their average values

Figure 5: Indoor temperature dynamics under dynamic pricing over a 45-day period. In this experiment, dynamic prices are computed based on the average outside temperature and available renewables, and tested over days with new realizations of outside temperature and renewable availability

Bibliography

- Daniel Adelman and Canan Uçkun. Dynamic electricity pricing to smart homes. *Operations research*, 67(6):1520–1542, 2019. [3](#), [5](#)
- Vishal V Agrawal and Şafak Yücel. Design of electricity demand-response programs. *Management Science*, 68(10):7441–7456, 2022. [6](#)
- Hunt Allcott. Rethinking real-time electricity pricing. *Resource and Energy Economics*, 33(4):820–842, 2011a. [3](#)
- Hunt Allcott. Social norms and energy conservation. *Journal of Public Economics*, 95(9-10):1082–1095, 2011b. [6](#)
- Zvi Artstein. On the calculus of closed set-valued functions. *Indiana University Mathematics Journal*, 24(5):433–441, 1974. [11](#)
- Zvi Artstein and Richard A Vitale. A strong law of large numbers for random compact sets. *The Annals of Probability*, pages 879–882, 1975. [10](#)
- Shiri Artstein-Avidan, Apostolos Giannopoulos, and Vitali D Milman. *Asymptotic Geometric Analysis, Part I*, volume 202. American Mathematical Soc., 2015. [11](#)
- Robert J Aumann. Integrals of set-valued functions. *Journal of mathematical analysis and applications*, 12(1):1–12, 1965. [10](#), [11](#)
- Marc Beaudin and Hamidreza Zareipour. Home energy management systems: A review of modelling and complexity. *Renewable and Sustainable Energy Reviews*, 45:318–335, 2015. [2](#), [7](#)
- Ágnes Bellay. Measurability of set-valued functions. *Periodica Polytechnica Electrical Engineering (Archives)*, 30(1):55–63, 1986. [10](#)

- Lori Bird, Michael Milligan, and Debra Lew. Integrating variable renewable energy: Challenges and solutions. Technical report, National Renewable Energy Lab.(NREL), Golden, CO (United States), 2013. [1](#)
- Juan Caballero-Pena, Cristian Cadena-Zarate, Alejandro Parrado-Duque, and German Osma-Pinto. Distributed energy resources on distribution networks: A systematic review of modelling, simulation, metrics, and impacts. *International Journal of Electrical Power & Energy Systems*, 138:107900, 2022. [2](#)
- Yiling Chen, Yang Liu, and Chara Podimata. Learning strategy-aware linear classifiers. *Advances in Neural Information Processing Systems*, 33:15265–15276, 2020. [5](#)
- Felipe Cordera, Rodrigo Moreno, and Fernando Ordoñez. Unit commitment problem with energy storage under correlated renewables uncertainty. *Operations Research*, 71(6):1960–1977, 2023. [1](#)
- Michael A Crew, Chitru S Fernando, and Paul R Kleindorfer. The theory of peak-load pricing: A survey. *Journal of regulatory economics*, 8:215–248, 1995. [5](#)
- Kaitlin Daniels and Ruben Lobel. Demand response in electricity markets: Voluntary and automated curtailment contracts. *Available at SSRN 2505203*, 2014. [6](#)
- Paul Denholm, Matthew O’Connell, Gregory Brinkman, and Jennie Jorgenson. Overgeneration from solar energy in california. a field guide to the duck chart. Technical report, National Renewable Energy Lab.(NREL), Golden, CO (United States), 2015. [4](#)
- John C Duchi, Michael I Jordan, Martin J Wainwright, and Andre Wibisono. Optimal rates for zero-order convex optimization: The power of two function evaluations. *IEEE Transactions on Information Theory*, 61(5):2788–2806, 2015. [16](#)
- Ahmad Faruqui, Dan Harris, and Ryan Hledik. Unlocking the € 53 billion savings from smart meters in the eu: How increasing the adoption of dynamic tariffs could make or break the eu’s smart grid investment. *Energy Policy*, 38(10):6222–6231, 2010. [2](#)
- Ali Fattahi, Sriram Dasu, and Reza Ahmadi. Peak-load energy management by direct load control contracts. *Management Science*, 69(5):2788–2813, 2023. [6](#)
- Eric J Friedman and Shmuel S Oren. The complexity of resource allocation and price mechanisms under bounded rationality. *Economic Theory*, 6(2):225–250, 1995. [3](#)
- Radu Godina, Eduardo MG Rodrigues, Edris Pouresmaeil, João CO Matias, and João PS Catalão. Model predictive control home energy management and optimization strategy with demand response. *Applied Sciences*, 8(3):408, 2018. [2](#)
- Gautam Gowrisankaran, Stanley S Reynolds, and Mario Samano. Intermittency and the value of renewable energy. *Journal of Political Economy*, 124(4):1187–1234, 2016. [1](#)
- Elizabeth V Hobman, Elisha R Frederiks, Karen Stenner, and Sarah Meikle. Uptake and usage of cost-reflective electricity pricing: Insights from psychology and behavioural economics. *Renewable and Sustainable Energy Reviews*, 57:455–467, 2016. [3](#)

- Semich Impram, Secil Varbak Nese, and Bülent Oral. Challenges of renewable energy penetration on power system flexibility: A survey. *Energy Strategy Reviews*, 31:100539, 2020. ISSN 2211-467X. doi: <https://doi.org/10.1016/j.esr.2020.100539>. URL <https://www.sciencedirect.com/science/article/pii/S2211467X20300924>. 1
- Na Li, Lijun Chen, and Steven H Low. Optimal demand response based on utility maximization in power networks. In *2011 IEEE power and energy society general meeting*, pages 1–8. IEEE, 2011. 7
- Andreu Mas-Colell, Michael D. Whinston, and Jerry R. Green. *Microeconomic Theory*. Oxford University Press, New York, 1995. ISBN 9780195073409. 3
- Efstathios E Michaelides. Fossil fuel substitution with renewables for electricity generation—effects on sustainability goals. *European Journal of Sustainable Development Research*, 4(1):em0111, 2019. 1
- Evan Munro. Treatment allocation with strategic agents. *Management Science*, forthcoming, 2024. 5
- Office of Science and Technology Policy. Climate and energy implications of crypto-assets in the united states. Technical report, The White House, September 2022. 2
- Opinion Dynamics. 2022 flex alert evaluation draft report. Technical report, California Public Utilities Commission, 2024. 2
- Juan Perdomo, Tijana Zrnic, Celestine Mendler-Dünner, and Moritz Hardt. Performative prediction. In *International Conference on Machine Learning*, pages 7599–7609. PMLR, 2020. 5
- Heikki Peura and Derek W Bunn. Dynamic pricing of peak production. *Operations Research*, 63(6):1262–1279, 2015. 5
- R Tyrrell Rockafellar and Roger J-B Wets. *Variational analysis*, volume 317. Springer Science & Business Media, 2009. 10
- Roshni Sahoo and Stefan Wager. Policy learning with competing agents. *arXiv preprint arXiv:2204.01884*, 2022. 5
- Ohad Shamir. On the complexity of bandit and derivative-free stochastic convex optimization. In *Conference on Learning Theory*, pages 3–24. PMLR, 2013. 16
- Alexander Shapiro, Darinka Dentcheva, and Andrzej Ruszczyński. *Lectures on stochastic programming: modeling and theory*. SIAM, 2021. 13, 28
- Pierluigi Siano. Demand response and smart grids—a survey. *Renewable and sustainable energy reviews*, 30:461–478, 2014. 2
- Canan Uckun. *Dynamic electricity pricing for smart homes*. The University of Chicago, 2012. 5
- U.S. Energy Information Administration. Annual energy outlook 2023. 2023. URL <https://www.eia.gov/outlooks/aeo/>. 2

- Richard A Vitale. The brunn-minkowski inequality for random sets. *Journal of multivariate analysis*, 33(2):286–293, 1990. 10
- Stefan Wager and Kuang Xu. Experimenting in equilibrium. *Management Science*, 67(11):6694–6715, 2021. 16
- Eric Webb, Owen Q Wu, and Kyle Cattani. Coordinating energy efficiency and incentive-based demand response. *Kelley School of Business Research Paper*, (16-68), 2019. 6
- Ji Hoon Yoon, Ross Bladick, and Atila Novoselac. Demand response for residential buildings based on dynamic price of electricity. *Energy and Buildings*, 80:531–541, 2014. 2
- Bin Zhou, Wentao Li, Ka Wing Chan, Yijia Cao, Yonghong Kuang, Xi Liu, and Xiong Wang. Smart home energy management systems: Concept, configurations, and scheduling strategies. *Renewable and Sustainable Energy Reviews*, 61:30–40, 2016. 2, 7
- Xinyang Zhou, Emiliano Dall’Anese, Lijun Chen, and Andrea Simonetto. An incentive-based online optimization framework for distribution grids. *IEEE Transactions on Automatic Control*, 63(7):2019–2031, 2017. 3, 5, 8
- Xinyang Zhou, Emiliano Dall’Anese, and Lijun Chen. Online stochastic optimization of networked distributed energy resources. *IEEE Transactions on Automatic Control*, 65(6):2387–2401, 2019. 5

A Proofs

A.1 Proof of Proposition 1

An indifference set R with parameters (a, b) can be reformulated as

$$R = \{(wa, (1-w)b) : w \in [0, 1]\} . \quad (33)$$

For a price signal $p = (p_1, p_2)$, each HEMS solves the following optimization

$$w^* = \arg \min_{w \in [0, 1]} \{wap_1 + (1-w)bp_2\} .$$

This gives the consumption profile $q(p)$ given in (3) as

$$q(p) = (w^*a, (1-w^*)b) .$$

In this case, the optimal solution w^* is easy to characterize and is given by

$$w^* = \begin{cases} 1, & ap_1 < bp_2, \\ [0, 1], & ap_1 = bp_2, \\ 0, & ap_1 > bp_2. \end{cases}$$

We suppose that users when they are indifferent, i.e., when $ap_1 = bp_2$, they select period one ($w^* = 1$). For an indifference set R_i with parameters (a_i, b_i) this yields

$$q_i(p) = \left(\mathbb{I}(a_i p_1 \leq b_i p_2) a_i, \mathbb{I}(a_i p_1 > b_i p_2) b_i \right) .$$

Having $\bar{q} = \frac{1}{n} \sum_{i=1}^n q_i(p)$, the average grid cost function for the price p is $\|\bar{q}\|_\infty$, this allows us to characterize the grid risk under the price (p_1, p_2) as the following:

$$\hat{R}_n^{\text{PM}}(p) = \frac{1}{n} \max \left(\sum_{i=1}^n \mathbb{I}(a_i p_1 \leq b_i p_2) a_i, \sum_{i=1}^n \mathbb{I}(a_i p_1 > b_i p_2) b_i \right) .$$

The above formulation reveals that the grid cost function is scale-invariant with respect to price $p = (p_1, p_2)$, where for any $c > 0$, using cp yields the same grid cost value. In addition, if $p_1 p_2 \leq 0$, then it is straightforward to observe that by having the non-positive element to zero, we obtain the same grid risk value. Put all together, to obtain the best price signal, we can focus on the following two classes of prices: i) all p that $p_1 + p_2 = 1$, for $p_1, p_2 \geq 0$, and ii) all p that $p_1 + p_2 = -1$, for $p_1, p_2 \leq 0$. The first class can be parametrized by a one-dimensional parameter $0 \leq z \leq 1$ where $p_1 = z$ and $p_2 = (1-z)$, using this in the above yields

$$U_n^+ = \min_{0 \leq z \leq 1} U_n^+(z), \quad U_n^+(z) = \frac{1}{n} \max \left(\sum_{i=1}^n \mathbb{I}(a_i z \leq b_i (1-z)) a_i, \sum_{i=1}^n \mathbb{I}(a_i z > b_i (1-z)) b_i \right) .$$

In addition, for the class of price signals $p_1 + p_2 = -1$ with $p_1, p_2 \leq 0$, we can consider $p_1 = -z$, $p_2 = -1+z$ for $z \in [0, 1]$, using this in the formulation of $\hat{R}_n^{\text{PM}}(p)$ brings us

$$U_n^- = \min_{0 \leq z \leq 1} U_n^-(z), \quad U_n^-(z) = \frac{1}{n} \max \left(\sum_{i=1}^n \mathbb{I}(-a_i z \leq b_i (-1+z)) a_i, \sum_{i=1}^n \mathbb{I}(-a_i z > b_i (-1+z)) b_i \right)$$

Combining the above two classes of prices, then we can consider

$$\min_p \widehat{R}_n^{\text{PM}}(p) = \min_{z \in [0,1]} U_n(z), \quad U_n(z) = \min(U_n^+(z), U_n^-(z)).$$

We then focus on computing the risk of the direct method. For this end, we recall the indifference set formulation (33) and let the user i be parameterized by $w_i \in [0, 1]$, in this case we arrive at

$$\widehat{R}_n^{\text{DM}} = \min_{w_i \in [0,1], \forall i \in [n]} \left\| \frac{1}{n} \sum_{i=1}^n \begin{bmatrix} w_i a_i \\ (1-w_i) b_i \end{bmatrix} \right\|_{\ell_\infty}.$$

We next use the dual formulation of ℓ_∞ -norm to get

$$\widehat{R}_n^{\text{DM}} = \min_{w_i \in [0,1], \forall i \in [n]} \max_{\|r\|_{\ell_1} \leq 1} \frac{1}{n} \sum_{i=1}^n (r_1 w_i a_i + r_2 (1-w_i) b_i).$$

Given that the above objective function is bilinear in r and w_i 's, we can change min/max with max/min and arrive at

$$\widehat{R}_n^{\text{DM}} = \max_{\|r\|_{\ell_1} \leq 1} \min_{w_i \in [0,1], \forall i \in [n]} \frac{1}{n} \sum_{i=1}^n (r_1 w_i a_i + r_2 (1-w_i) b_i).$$

As the objective function is decoupled with respect to variables w_i , we can take the minimization inside and get

$$\widehat{R}_n^{\text{DM}} = \max_{\|r\|_{\ell_1} \leq 1} \frac{1}{n} \sum_{i=1}^n \min_{w_i \in [0,1]} (r_1 w_i a_i + r_2 (1-w_i) b_i).$$

The inside optimization is easy to characterize, where the optimal solution is given by

$$w_i^* = \begin{cases} 1, & r_1 a_i \leq r_2 b_i, \\ 0, & r_1 a_i > r_2 b_i. \end{cases}$$

Using this yields

$$\widehat{R}_n^{\text{DM}} = \max_{\|r\|_{\ell_1} \leq 1} \frac{1}{n} \sum_{i=1}^n (r_1 a_i \mathbb{I}(r_1 a_i \leq r_2 b_i) + r_2 b_i \mathbb{I}(r_1 a_i > r_2 b_i)).$$

In the next step, we first note that given the non-negative values for a_i, b_i , it is easy to observe that r_1, r_2 to maximize the above objective must be non-negative, and the constraint can be written as $r_1 + r_2 = 1$, for $r_1, r_2 \geq 0$. In addition, it can be seen that the optimal r^* must be on the boundary of unit ℓ_1 -ball, otherwise if $\|r^*\|_{\ell_1} < 1$, we can easily consider $\tilde{r} = r^*/\|r^*\|_{\ell_1}$ and strictly increase the value of the objective function. This enables us to focus on all r values that $r_1 + r_2 = 1$, by considering $z \in [0, 1]$ and letting $r_1 = z, r_2 = (1-z)$, this brings us

$$\widehat{R}_n^{\text{DM}} = \max_{0 \leq z \leq 1} \frac{1}{n} \sum_{i=1}^n \left((1-z) b_i \mathbb{I}((1-z) b_i < z a_i) + z a_i \mathbb{I}((1-z) b_i \geq z a_i) \right).$$

This completes the proof.

A.2 Characterizing \mathcal{P}

Lemma 9. For the grid const function $\rho(\cdot)$ given in Assumption 2, let

$$\mathcal{P} \triangleq \left\{ p \in \mathbb{R}^d : p^\top r \leq \rho(r), \quad \forall r \in \mathbb{R}^d \right\}.$$

Then, \mathcal{P} is a compact convex set, and its support function is $\rho(\cdot)$. More precisely, we have

$$\rho(q) = \max_{z \in \mathcal{P}} z^\top q, \quad \forall q \in \mathbb{R}^d.$$

In addition, ρ is Lipschitz continuous with parameter $\|\mathcal{P}\|$, where

$$|\rho(q_1) - \rho(q_2)| \leq \|\mathcal{P}\| \|q_1 - q_2\|, \quad \forall q_1, q_2 \in \mathbb{R}^d.$$

Proof. For the boundedness of \mathcal{P} , note that if $\tilde{p} \in \mathcal{P}$ by using $r = \tilde{p}$ we arrive at $\|\tilde{p}\|_2^2 \leq \rho(\tilde{p})$. Using positive homogeneity of ρ brings us

$$\|\tilde{p}\|_2 \leq \frac{\rho(\tilde{p})}{\|\tilde{p}\|_2} = \rho\left(\frac{\tilde{p}}{\|\tilde{p}\|_2}\right) \leq \sup_{x \in \mathbb{S}^{d-1}} \rho(x).$$

Given the continuity of ρ , on the unit sphere \mathbb{S}^{d-1} we realize that ρ is bounded. This implies that there exists a real-valued M such that $\sup_{x \in \mathbb{S}^{d-1}} \rho(x) \leq M$. Using this in the above, we get that for every $\tilde{p} \in \mathcal{P}$ we have $\|\tilde{p}\| \leq M$, this establishes the boundedness of \mathcal{P} . In addition, if $\{p_n\}_{n \geq 1}$ is a sequence of points converging to p such that $p_n \in \mathcal{P}$, it is straightforward to get that $p \in \mathcal{P}$, showing the closeness of \mathcal{P} . Put all together, it can be observed that \mathcal{P} is a compact set.

To show convexity, note that if $p_1, p_2 \in \mathcal{P}$, then for every $\alpha \in (0, 1)$, given that $p_1^\top r \leq \rho(r)$, and $p_2^\top r \leq \rho(r)$, then we have that $(\alpha p_1 + (1 - \alpha)p_2)^\top r \leq \rho(r)$, so $\alpha p_1 + (1 - \alpha)p_2 \in \mathcal{P}$.

We next show that the support function of \mathcal{P} is $\rho(\cdot)$. For this end, define the function $f(r) = \sup_{p \in \mathcal{P}} (p^\top r - \rho(r))$. For a fixed value of r , and a positive α , we have the following

$$\begin{aligned} f(\alpha r) &= \sup_{p \in \mathcal{P}} (p^\top (\alpha r) - \rho(\alpha r)) \\ &= \alpha \sup_{p \in \mathcal{P}} (p^\top r - \rho(r)) \\ &= \alpha f(r). \end{aligned}$$

where in the penultimate relation we used the homogeneity of ρ . As this holds for every $\alpha \geq 0$ then we realize that $f(r)$ must be either $-\infty, 0$, or $+\infty$. By definition of \mathcal{P} , if $p \in \mathcal{P}$, we know that $f(r) \leq 0$, removing the $+\infty$ choice, implying that $f(r)$ can be 0 or $-\infty$. We also have

$$\begin{aligned} \rho(r) &= \|r\| \rho\left(\frac{r}{\|r\|}\right) \\ &\leq \|r\| \sup_{x \in \mathbb{S}^{d-1}} \rho(x) \\ &\leq M \|r\|. \end{aligned}$$

In addition, as $|\sup_{p \in \mathcal{P}} p^\top r| \leq \|r\| \|\mathcal{P}\| \leq M\|r\|$, we realize that $-2M\|r\| \leq f(r) \leq 0$, therefore $f(r)$ for every fixed r can not be $-\infty$, therefore it is zero. This implies that $\sup_{p \in \mathcal{P}} p^\top r = \rho(r)$, meaning that $\rho(\cdot)$ is the support function of \mathcal{P} . For the Lipschitz property, for $i = 1, 2$ let

$$p_i^* = \arg \min_{p \in \mathcal{P}} p^\top q_i.$$

Using this definition brings us

$$\begin{aligned} \rho(q_1) - \rho(q_2) &= q_1^\top p_1^* - q_2^\top p_2^* \\ &= q_1^\top (p_1^* - p_2^*) + (q_1 - q_2)^\top p_2^* \\ &\leq (q_1 - q_2)^\top p_2^* \\ &\leq \|\mathcal{P}\| \|q_1 - q_2\|. \end{aligned}$$

By a similar chain of inequalities it can be shown that $-\|\mathcal{P}\| \|q_1 - q_2\| \leq \rho(q_1) - \rho(q_2)$, this completes the proof. \square

A.3 Proof of Theorem 5

We have

$$\Theta_i(z^*) = \left\{ q \in \mathbf{R}_i : q^\top z^* = h(z^*; \mathbf{R}_i) \right\}. \quad (34)$$

In the next step, by the Levin–Valadier theorem [Shapiro et al., 2021, Theorem 7.22], given that $h(\cdot; \mathbf{R}_i)$ is concave we have

$$\partial_z h(z^*; \mathbf{R}_i) = \text{conv}(\Theta_i(z^*)).$$

In addition, under Assumption 3, we have that $h(\cdot; \mathbf{R}_i)$ is differentiable at z^* almost surely. By using this in the above, we realize that $\Theta_i(z^*)$ must be a singleton, given by $\Theta_i(z^*) = \{\nabla h(z^*; \mathbf{R}_i)\}$. We now move to prove the second part. From the definition of $H(\cdot)$ we know that $H(z^*) = h(z^*; \mathbb{E}[\mathbf{R}])$, therefore $\Theta(z^*)$ can be expressed as

$$\Theta(z^*) = \{q : q \in \mathbb{E}[\mathbf{R}_i], q \cdot z^* = H(z^*)\}. \quad (35)$$

We once more apply the Levin–Valadier Theorem for the concave function $H(z)$ to arrive at

$$\partial H(z^*) = \text{conv}(\Theta(z^*)).$$

As $H(\cdot)$ is differentiable at z^* as established in Theorem 4, $\Theta(z^*)$ must be a singleton, and $\Theta(z^*) = \{\nabla H(z^*)\}$, therefore $\bar{q}(z^*) = \nabla H(z^*)$. In addition, from Lemma 2 we have $\mathbb{E}[h(z; \mathbf{R}_i)] = h(z; \mathbb{E}[\mathbf{R}_i])$, therefore $H(z) = \mathbb{E}[h(z; \mathbf{R}_i)]$. We then use the concave property of $h(\cdot; \mathbf{R}_i)$, and $H(\cdot)$ in conjunction with Theorem 7.46 of Shapiro et al. [2021] to get $\nabla H(z^*) = \mathbb{E}[\nabla h(z^*; \mathbf{R}_i)]$. Combining this result with $\Theta_i(z^*) = \{\nabla h(z^*; \mathbf{R}_i)\}$ implies that $\mathbb{E}[\Theta_i(z^*)] = \Theta(z^*)$.

A.4 Proof of Corollary 6

From Theorem 5 we have that $\bar{q}(z^*)$ is the unique solution for a consumer HEMS optimization of average indifference set $\mathbb{E}[\mathbf{R}]$, formally

$$\bar{q}(z^*) = \arg \min_{\mathbb{E}[\mathbf{R}]} q^\top z^*.$$

In addition, from the above optimization characterization we know that $\bar{q}(z^*) \in \partial H(z^*)$ (see arguments used in (19)). Given the differentiability of $H(\cdot)$ at z^* (see Assumption 3), we obtain $\bar{q}(z^*) = \nabla H(z^*)$. We next write the first order optimality condition for the concave function $H(z) - z^\top q_0$ over \mathcal{P} , we arrive at the following

$$(\nabla H(z^*) - q_0)^\top (z - z^*) \leq 0, \quad \forall z \in \mathcal{P}.$$

This reads as

$$z^{*\top} (\nabla H(z^*) - q_0) \geq z^\top (\nabla H(z^*) - q_0), \quad \forall z \in \mathcal{P}.$$

As this holds for all $z \in \mathcal{P}$, we obtain

$$z^{*\top} (\nabla H(z^*) - q_0) \geq \max_{z \in \mathcal{P}} z^\top (g^* - q_0).$$

In addition, the above maximization is achieved at $z^* \in \mathcal{P}$, therefore it must be an equality, and can be rewritten as

$$z^{*\top} (\nabla H(z^*) - q_0) = \max_{z \in \mathcal{P}} z^\top (\nabla H(z^*) - q_0).$$

In the next step, we deploy Lemma 9 in the above to obtain

$$z^{*\top} (\nabla H(z^*) - q_0) = \rho(\nabla H(z^*) - q_0). \quad (36)$$

We next use $\bar{q}(z^*) = \nabla H(z^*)$ in the above, and this amounts to $U(z^*) = \rho(\bar{q}(z^*) - q_0)$. We next use $q_0 \notin \mathbb{E}[\mathbf{R}]$ to get that $\bar{q}(z^*) - q_0$ is not zero, accordingly $\rho(\bar{q}(z^*) - q_0)$ is not zero. Given that ρ is non-negative valued, therefore $\rho(\bar{q}(z^*) - q_0) > 0$. Plugging this into the above, yields $U(z^*) > 0$, and completes the proof.

A.5 Proof of Corollary 7

For a vector $u \in \mathbb{R}^d$, we adopt the following shorthand $u_+ = \max(u, 0)$, where the maximum is taken componentwise. We first claim that if $p \in \mathcal{P}$, then p_+ also belongs to \mathcal{P} . To show this, from Lemma 9 we must show that

$$p_+^\top r \leq \rho(r), \quad \forall r \in \mathbb{R}^d.$$

We first note that

$$\begin{aligned} p_+^\top r &= \sum_{\ell: p_\ell \geq 0} p_\ell^* r_\ell \\ &= \sum_{\ell: p_\ell \geq 0, r_\ell \leq 0} p_\ell^* r_\ell + \sum_{\ell: p_\ell^* \geq 0, r_\ell \geq 0} p_\ell^* r_\ell \\ &\leq \sum_{\ell: p_\ell^* \geq 0, r_\ell \geq 0} p_\ell^* r_\ell. \end{aligned}$$

We then consider r' where for $\ell \in [d]$, its ℓ -th coordinate is defined as follows

$$r'_\ell = \begin{cases} r_\ell, & p_\ell \geq 0, r_\ell \geq 0, \\ 0, & \text{o.w.} \end{cases}$$

From the above formulation, it is easy to observe that $r'^{\top} p^* = \sum_{\ell: p_{\ell}^* \geq 0, r_{\ell} \geq 0} p_{\ell}^* r_{\ell}$, therefore by using this in the above we get

$$p_+^{\top} r \leq r'^{\top} p^* .$$

In addition, it is easy to observe that r' is such that either $0 \leq r'_{\ell} \leq r_{\ell}$, or $r'_{\ell} = 0$ when $r_{\ell} < 0$. Therefore, it satisfies the monotonicity condition, and therefore $\rho(r') \leq \rho(r)$. Put all together, we arrive at

$$p_+^{\top} r \leq r'^{\top} p^* \leq \rho(r') \leq \rho(r) ,$$

where $r'^{\top} p^* \leq \rho(r')$ follows from $p^* \in \mathcal{P}$. As this holds for all r , therefore p_+ must belong to \mathcal{P} . We now complete the argument and show that for p^* , if we consider $p = p_+$, then the objective function $H(p) - p^{\top} q_0 = \min_{\mathbb{E}[\mathbf{R}]} (q - q_0)^{\top} p$ will not decrease, compared to $p = p^*$. This in conjunction with the fact that $p_+^* \in \mathcal{P}$ implies that p^* must have all non-negative coordinates, and completes the proof. For this end, we consider $r = q - q_0$ for some $q \in \mathbb{E}[\mathbf{R}]$, we then have

$$\begin{aligned} r^{\top} p_+^* &= \sum_{\ell: p_{\ell}^* \geq 0} p_{\ell}^* r_{\ell} \\ &\geq \sum_{\ell} p_{\ell}^* r_{\ell} , \end{aligned}$$

where the last relation follows from the Assumption 4 that $q \geq q_0$ (componentwise), thus r has non-negative coordinates. This implies that $r^{\top} p_+^* \geq r^{\top} p^*$, therefore

$$\min_{\mathbb{E}[\mathbf{R}]} (q - q_0)^{\top} p_+^* \geq \min_{\mathbb{E}[\mathbf{R}]} (q - q_0)^{\top} p^* .$$

This completes the proof.

A.6 Proof of Theorem 8

For random convex sets $\{\mathbf{C}_i\}_{1 \leq i \leq N}$ in \mathfrak{C}_d , from the almost sure convergence result (12) we have

$$\lim_{n \rightarrow \infty} d_{\mathbb{H}} \left(\frac{1}{n} \bigoplus_{i=1}^n \mathbf{C}_i, \mathbb{E}[\mathbf{C}] \right) = 0 .$$

In addition, for two convex sets $C_1, C_2 \in \mathfrak{C}_d$, the Hausdorff distance between C_1, C_2 can be written as the infinity norm of their support functions, formally we have

$$d_{\mathbb{H}}(C_1, C_2) = \sup_{u \in \mathbb{S}^{d-1}} |\delta(u; C_1) - \delta(u; C_2)| .$$

Using this in the above, yields

$$\lim_{n \rightarrow \infty} \sup_{u \in \mathbb{S}^{d-1}} \left| \delta \left(u; \frac{1}{n} \bigoplus_{i=1}^N \mathbf{C}_i \right) - \delta(u; \mathbb{E}[\mathbf{C}]) \right| = 0 .$$

We next use the linearity of support functions for Minkowski sum, where formally for convex sets C_1, C_2 we have

$$\delta(u; C_1 \oplus C_2) = \delta(u; C_1) + \delta(u; C_2) , \quad \forall u \in \mathbb{S}^{d-1} .$$

This gives us

$$\lim_{n \rightarrow \infty} \sup_{u \in \mathbb{S}^{d-1}} \left| \frac{1}{n} \sum_{i=1}^n \delta(u; \mathbf{C}_i) - \delta(u; \mathbb{E}[\mathbf{C}]) \right| = 0. \quad (37)$$

We next use $h(z; \mathbf{R}) = -\delta(-z; \mathbf{R})$, in conjunction with the definition of $H(z) = h(z; \mathbb{E}[\mathbf{R}])$, and the fact that support function of a set and its convex hull are equal, i.e., $\delta(z; \mathbf{R}) = \delta(z; \text{conv}(\mathbf{R}))$. This brings us

$$\lim_{n \rightarrow \infty} \sup_{u \in \mathbb{S}^{d-1}} \left| \frac{1}{n} \sum_{i=1}^n h(u; \mathbf{R}_i) - H(u) \right| = 0.$$

We next deploy the positive homogeneity of function $h(\cdot, \mathbf{R})$, and its mean-field value $H(\cdot)$ to obtain

$$\begin{aligned} \sup_{z \in \mathcal{P}} \left| \frac{1}{n} \sum_{i=1}^n h(z; \mathbf{R}_i) - H(z) \right| &= \sup_{z \in \mathcal{P}} \|z\| \left| \frac{1}{n} \sum_{i=1}^n h\left(\frac{z}{\|z\|}; \mathbf{R}_i\right) - H\left(\frac{z}{\|z\|}\right) \right| \\ &\leq \sup_{z \in \mathcal{P}} \|z\| \sup_{u \in \mathbb{S}^{d-1}} \left| \frac{1}{n} \sum_{i=1}^n h(u; \mathbf{R}_i) - H(u) \right|. \end{aligned}$$

Using this in the above in along with the boundedness of $\|\mathcal{P}\|$ (see Lemma 9) gives us

$$\lim_{n \rightarrow \infty} \sup_{z \in \mathcal{P}} \left| \widehat{H}_n(z) - H(z) \right| = 0. \quad (38)$$

We then let $z^* \in \arg \max_{\mathcal{P}} (H(z) - z^\top q_0)$, it can be observed that $(H(z^*) - q_0^\top z^*) = \mathbf{R}^{\text{DM}}(q_0)$. In the next step, having established the uniform convergence of the sample average of users's cost function to their mean-field function $H(\cdot)$, we write the following chain of relations with the new notation $q_{0,n} = Q_0/n$:

$$\begin{aligned} (H(z^*) - q_0^\top z^*) - (H(\widehat{z}_n) - \widehat{z}_n^\top q_0) &= (H(z^*) - q_0^\top z^*) - (\widehat{H}_n(z^*) - q_{0,n}^\top z^*) \\ &\quad + (\widehat{H}_n(z^*) - q_{0,n}^\top z^*) - (\widehat{H}_n(\widehat{z}_n) - q_{0,n}^\top \widehat{z}_n) \\ &\quad + (\widehat{H}_n(\widehat{z}_n) - q_{0,n}^\top \widehat{z}_n) - (H(\widehat{z}_n) - \widehat{z}_n^\top q_0). \end{aligned}$$

We next use the definition of \widehat{z}_n as maximizer of $\widehat{H}_n(z) - z^\top q_{0,n}$ to get

$$\begin{aligned} (H(z^*) - q_0^\top z^*) - (H(\widehat{z}_n) - \widehat{z}_n^\top q_0) &\leq (H(z^*) - q_0^\top z^*) - (\widehat{H}_n(z^*) - q_{0,n}^\top z^*) \\ &\quad + (\widehat{H}_n(\widehat{z}_n) - q_{0,n}^\top \widehat{z}_n) - (H(\widehat{z}_n) - \widehat{z}_n^\top q_0). \end{aligned}$$

Finally, we deploy the uniform convergence result of (38) in along with almost sure convergence $Q_0/n \rightarrow q_0$ to realize that the above right-hand side in the mean-field is non-positive, thereby

$$\lim_{n \rightarrow \infty} (H(\widehat{z}_n) - \widehat{z}_n^\top q_0) \geq H(z^*) - q_0^\top z^*.$$

Given that z^* is a maximizer of $H(z) - q_0^\top z$ over \mathcal{P} , combining this with the above we realize that with probability one the following holds

$$\lim_{n \rightarrow \infty} (H(\widehat{z}_n) - q_0^\top \widehat{z}_n) = H(z^*) - q_0^\top z^*. \quad (39)$$